CHAPTER 3

Oscillatory Motion and Chaos

Examples of oscillatory phenomena can be found in many areas of physics, including the motion of electrons in atoms, the behavior of currents and voltages in electronic circuits, and planetary orbits. Perhaps the simplest mechanical system that exhibits such motion is a pendulum, consisting of a mass that is connected by a string to some sort of support so that it is able to swing freely in response to the force of gravity. In the idealized case, ignoring friction and assuming that the angle the string makes with the vertical is small, such a pendulum undergoes what is known as simple harmonic motion. The main features of this motion are common to many types of oscillating systems, making it a paradigm in elementary physics textbooks. However, elementary-level treatments usually do not consider the behavior of a *real* pendulum, that is, a pendulum that has some friction, that is driven by an external force, and that is allowed to swing to large angles. The motion of such a pendulum exhibits many features not found in the simple harmonic case. Perhaps the most important of these features is the possibility of chaotic behavior, which is the central topic of this chapter.

In the next several sections we will explore some of the interesting effects that occur in real oscillatory systems. We begin with a simple pendulum and consider how to treat simple harmonic motion numerically. We then generalize our pendulum model to include the effects of friction and nonlinearities and find that they give rise to the possibility of chaotic behavior. While the term chaos probably has some intuitive meaning for all of us, it is not easy to give a precise definition of this notion (especially one that would make a physicist or a mathematician happy). We will, therefore, spend some time in formulating such a definition, and this will lead us to consider several key issues. The remainder of the chapter is devoted to the study of a variety of other systems that exhibit chaotic behavior.

3.1 SIMPLE HARMONIC MOTION

One example of a simple pendulum is a particle of mass m connected by a massless string to a rigid support. We let θ be the angle that the string makes with the vertical and assume that the string is always taut, as in Figure 3.1. We also assume that there are only two forces acting on the particle, gravity and the tension of the string. It is convenient to consider the components of these forces parallel and perpendicular to the string. The parallel forces add to zero, since we assume that the string doesn't stretch or break, while the force perpendicular to the string is given by

$$F_\theta = -mg\sin\theta\,, \tag{3.1}$$

where g is the acceleration due to gravity, and the minus sign reminds us that the force is always opposite to the displacement from the vertical, where $\theta = 0$.

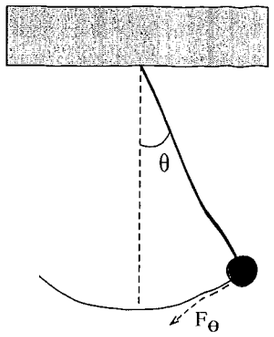

FIGURE 3.1: A simple pendulum, consisting of a mass connected by a string to a fixed point on a support, such as a ceiling.

Newton's second law tells us that this force is equal to the mass times the acceleration of the particle along the circular arc that is the particle's trajectory, that is, $F_\theta = md^2s/dt^2$. The displacement along this arc is $s = \ell\,\theta$, where ℓ is the length of the string. If we now assume that θ is always small so that $\sin\theta \approx \theta$, we obtain the (probably familiar) equation of motion

$$\frac{d^2\theta}{dt^2} = -\frac{g}{\ell}\theta\,. \tag{3.2}$$

This is the central equation of simple harmonic motion. It is easy to verify that it has the general solution

$$\theta = \theta_0\,\sin(\Omega t + \phi)\,, \tag{3.3}$$

where $\Omega = \sqrt{g/\ell}$, and θ_0 and ϕ are constants that depend on the initial displacement and velocity of the pendulum. We see that the motion of a simple pendulum is indeed very simple. The oscillations are sinusoidal with time and continue forever without decaying, which is not surprising since there is no friction in the model. The oscillations have an angular frequency, Ω, which is a function of the length of the string (and g, of course), but is independent of m and the amplitude of the motion.

We now consider a numerical approach to this problem. You might wonder why this is necessary, since the analytic solution is already in hand. However, this is just a warm-up exercise, as we will soon be turning our attention to slightly more complicated oscillatory problems for which exact results are not available. Our basic equation of motion is the second-order differential equation (3.2), which we want to solve for θ as a function of t. It is convenient to rewrite this as two first-order differential equations

$$\begin{aligned}\frac{d\omega}{dt} &= -\frac{g}{\ell}\theta\,, \\ \frac{d\theta}{dt} &= \omega\,,\end{aligned} \tag{3.4}$$

where ω is the angular velocity of the pendulum. This should look familiar, as we took a very similar approach in the projectile problems in Chapter 2. There we used the Euler method to solve a similar set of equations, so let us consider the same algorithm here. We convert (3.4) into difference equations, using a time step Δt so that time is discretized with $t = i\Delta t$, where i is an integer. Letting θ_i and ω_i be the numerically approximated angular displacement and velocity of the pendulum at time step i, the equations in (3.4) become

$$\begin{aligned} \omega_{i+1} &= \omega_i - \frac{g}{\ell}\theta_i\,\Delta t\,, \\ \theta_{i+1} &= \theta_i + \omega_i\,\Delta t\,. \end{aligned} \tag{3.5}$$

These are closely analogous to the difference equations we obtained when using the Euler method in Chapters 1 and 2. As in those problems, we use θ_i and ω_i (i.e., values at time step i) to estimate the values at step $i+1$, then repeat the process for steps $i+2$, $i+3$, ...

In constructing a program to implement this approach, we can use arrays to hold the values of θ, ω, and t, or we might store these results in a file as they are calculated. Either way, the heart of the calculation is the subroutine `euler_calculate` given below. This routine computes θ and ω with the Euler method in (3.5).

EXAMPLE 3.1 Pseudocode for subroutine `euler_calculate`

- For each time step i calculate ω and θ at time step $i+1$.
  - ▷ $\omega_{i+1} = \omega_i - (g/\ell)\theta_i\Delta t$
  - ▷ $\theta_{i+1} = \theta_i + \omega_i\Delta t$
  - ▷ $t_{i+1} = t_i + \Delta t$
  - ▷ Repeat for the desired number of time steps.

Some results from a program based on the Euler method are shown in Figure 3.2. The behavior we see there is very peculiar; while the motion is basically oscillatory, the amplitude of the oscillations *grows* with time. This is contrary to the exact solution, (3.3), and should also be at odds with your intuition. Since the model does not contain any source of energy nor does it include any friction, the total energy of the pendulum should remain constant. However, our program doesn't seem to appreciate this fact!

It turns out that the difficulty lies with our use of the Euler method. As was emphasized when we first introduced this method in Chapter 1, it provides us with an approximate estimate of the solution to our differential equation, (3.2). Again, the emphasis is on the word *approximate*. We have already mentioned that the errors involved in using the Euler method become smaller as the time step is made smaller. You might, therefore, think that the erroneous behavior seen in Figure 3.2 could be corrected by simply using a smaller value of Δt in our program. Reducing Δt will indeed make the errors smaller, but it turns out that the energy of the pendulum will increase with time for *any* nonzero value of Δt.

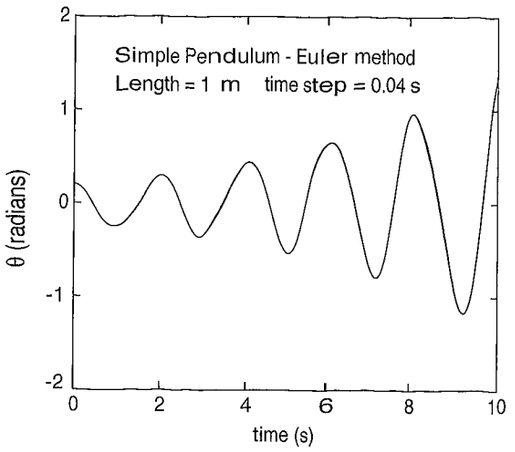

FIGURE 3.2: θ as a function of time for our simple pendulum, calculated using the Euler method with program pendulum. Here, and in most of the other figures in this chapter, we have connected the calculated values with solid lines.

At this point you might sense a contradiction. If the errors get smaller when Δt is reduced, how can the calculated behavior be defective for all values of Δt? The results in Figure 3.2 show that for our Euler solution both the amplitude of the oscillations and the total energy increase with time. If the calculation were repeated with a smaller value of Δt (a job we will leave for the exercises), the *rate* of this increase would be smaller. However, for all nonzero values of Δt we would find that the energy increases with time, and hence the Euler solution is, in that sense, always incorrect.

This is our first encounter with a numerical method that is inherently unstable. To see how this instability comes about we consider the total energy of the pendulum. This energy, E, is given by

$$E = \frac{1}{2}m\ell^2\omega^2 + mg\ell(1-\cos\theta)\,. \tag{3.6}$$

The first term is the kinetic energy, and is just $\frac{1}{2}mv^2$ where $v = \omega\ell$. The second term in (3.6) is the gravitational potential energy, and is equal to mgh where h is the height of the mass above the lowest point on its trajectory. In the limit of small θ the energy reduces to

$$E = \frac{1}{2}m\ell^2(\omega^2 + \frac{g}{\ell}\theta^2)\,. \tag{3.7}$$

Substituting ω_{i+1} and θ_{i+1} from the Euler method (3.5) into ω and θ in (3.7), the Euler result for the energy at time t_{i+1} is

$$E_{i+1} = E_i + \frac{1}{2}mg\ell\left(\omega_i^2 + \frac{g}{\ell}\theta_i^2\right)(\Delta t)^2\,. \tag{3.8}$$

Since the second term on the right is always positive, the energy of the Euler "solution" *always* increases with time, no matter how small we make Δt.

But if the Euler method is unstable in this way, how did we manage to get away with using it for the problems in Chapters 1 and 2? The answer to this is that a method can only be termed "suitable" or "unsuitable" (i.e., "good" or "not good") in the context of a particular problem. In the problems treated in Chapters 1 and 2 the Euler method also yielded (in most cases) solutions that did not quite conserve energy.[1] However, in those situations the errors were negligible on the scales relevant for those particular problems. In contrast, for problems involving oscillatory motion we often want to consider the behavior for many periods of oscillation. In order to be useful in such cases, a numerical method must conserve energy over the long haul.[2] The Euler method is not a good choice for these types of problems.

We are thus led to consider other methods for solving ordinary differential equations. This is such an important class of problems that we have devoted Appendix A to a discussion of several different numerical approaches, including the Runge-Kutta and Verlet methods. While those work well in dealing with the oscillatory problems encountered in this chapter, it turns out that a simple modification of the Euler method yields an algorithm that is also quite suitable. This modification yields what is known as the Euler-Cromer method, as Cromer was the first to carefully discuss the algorithm and show why it works. To appreciate the Euler-Cromer method, we reconsider our pendulum program. Given below is a *modified* version of the `calculate` subroutine.

EXAMPLE 3.2 Subroutine `euler_cromer_calculate` with the Euler-Cromer method

- For each time step i calculate ω and θ at time step $i+1$.
  - ▷ $\omega_{i+1} = \omega_i - (g/\ell)\theta_i \Delta t$
  - ▷ $\theta_{i+1} = \theta_i + \omega_{i+1}\Delta t$ (Note that ω_{i+1} is used to calculate θ_{i+1}.)
  - ▷ $t_{i+1} = t_i + \Delta t$
  - ▷ Repeat for the desired number of time steps.

The *only* change in this subroutine is emphasized by the added note in the above pseudocode, and can be appreciated as follows. With the Euler method, the *previous* value of ω and the *previous* value of θ are used to calculate the new values of both ω and θ. However, with the Euler-Cromer method, the *previous* values of ω and θ are used to calculate the new value of ω, but the *new* value of ω is used to calculate the new value of θ. This is such a minor change in the algorithm that you are probably surprised that it makes any difference. Indeed, for

[1] A notable exception was the constant acceleration problem considered in Chapter 1, for which the Euler method gives the exact solution.

[2] More precisely, the numerical algorithm must *itself* not contribute or remove energy from the system.

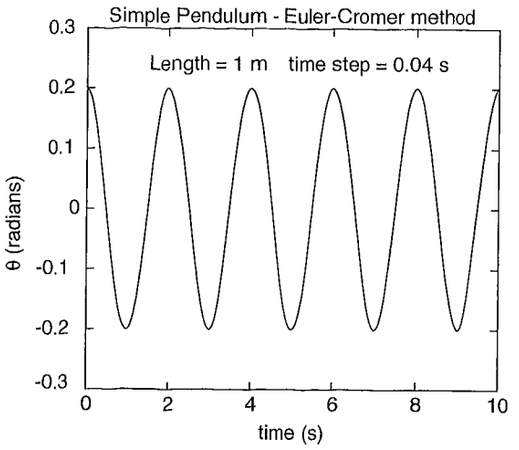

FIGURE 3.3: θ as a function of time for a simple pendulum calculated using the Euler-Cromer method.

many problems it makes no significant difference. However, for problems involving oscillatory motion the Euler-Cromer method conserves energy over each complete period of the motion,[3] and thus avoids the difficulties we found in Figure 3.2. Figure 3.3 shows a stable oscillation obtained with the Euler-Cromer algorithm (the parameters used here were the *same* as those used in the calculation shown in Figure 3.2). This numerical solution is very stable; these calculated oscillations would persist until our patience runs out. There are other numerical methods besides the Euler-Cromer algorithm that yield accurate solutions for oscillatory problems. Appendix A contains a description and discussion of the advantages and disadvantages of several other methods.

EXERCISES

3.1. Numerically investigate the stability of the Euler-Cromer method. Calculate the total energy, kinetic plus potential, of the pendulum as a function of time. Show that the energy is conserved over each complete cycle of the motion.

3.2. Repeat the previous problem using the Runge-Kutta method described in Appendix A. Compare the accuracy of the Runge-Kutta method with that of the Euler-Cromer algorithm using the same time step.

3.3. Use the Euler method to simulate the motion of a pendulum as in Figure 3.2. Study the behavior as a function of the step size, Δt, and show that the total energy always increases with time.

3.4. For simple harmonic motion, the general form for the equation of motion is

$$\frac{d^2x}{dt^2} = -k\,x^{\alpha}\,, \tag{3.9}$$

[3] For more on this see the exercises.

with $\alpha = 1$. This has the same form as (3.2), although the variables have different names. Begin by writing a program that uses the Euler-Cromer method to solve for x as a function of time according to (3.9), with $\alpha = 1$ (for convenience you can take $k = 1$). The subroutine described in this section can be modified to accomplish this. Show that the period of the oscillations is independent of the amplitude of the motion. This is a key feature of simple harmonic motion. Then extend your program to treat the case $\alpha = 3$. This is an example of an *anharmonic* oscillator. Calculate the period of the oscillations for several different amplitudes (amplitudes in the range 0.2 to 1 are good choices), and show that the period of the motion now depends on the amplitude. Give an intuitive argument to explain why the period becomes longer as the amplitude is decreased.

***3.5.** For the anharmonic oscillator of (3.9) in the previous exercise, it is possible to analytically obtain the period of oscillation for general values of α in terms of certain special functions. Do this, and describe how the relationship between the period and the amplitude depends on the value of α. Can you give a physical interpretation to the finding? *Hint:* If you multiply both sides of (3.9) by $\frac{dx}{dt}$ you can integrate with respect to t. This then leads to a relation between the velocity and x.

3.2 MAKING THE PENDULUM MORE INTERESTING: ADDING DISSIPATION, NONLINEARITY, AND A DRIVING FORCE

Let us now consider how we might make the simple pendulum in the previous section a bit more realistic. The equation of motion (3.2) describes a frictionless pendulum, so we begin by adding some damping. The manner in which friction enters the equations of motion depends on the origin of the friction. Possible sources of friction include the effective bearing where the string of the pendulum connects to the support, air resistance, etc. In many cases this damping force is proportional to the velocity, and that is the assumption we will make here.[4] The frictional force we will employ thus has the form $-q(d\theta/dt)$, since the velocity of the pendulum is $\ell(d\theta/dt)$. Here q is a parameter that measures the strength of the damping, and the minus sign guarantees that this force will always oppose the motion of the pendulum. Thus, the equation of motion for our damped pendulum has the form

$$\frac{d^2\theta}{dt^2} = -\frac{g}{\ell}\theta - q\frac{d\theta}{dt}, \tag{3.10}$$

where the second term on the right models the friction. Since this differential equation is still linear, we can solve it analytically just as we solved (3.2). The details of the solution can be found in many standard mechanics texts (such as the one by Marion and Thornton in the references), but in short, there are three regimes of distinct physical behavior. The first regime, called *underdamped*, occurs for sufficiently small friction, where the solution

$$\theta(t) = \theta_0 e^{-qt/2}\sin(\sqrt{\Omega^2 - q^2/4}\,t + \phi) \tag{3.11}$$

[4]Note, however, that other functional forms are possible. For example, in the case of air resistance, we noted in Chapter 2 that while the drag from air resistance is proportional to v for very small velocities, it varies as v^2 in many cases of practical interest. We will leave the investigation of the behavior with other forms for F_{friction} to the inquisitive reader.

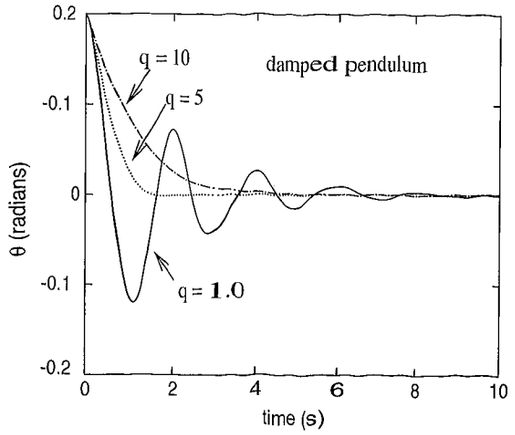

FIGURE 3.4: θ as a function of time for a damped pendulum for several different values of the damping, q, calculated using the Euler-Cromer method. Here we have taken $g = 9.8$ and $\ell = 1.0$. For $q = 5$ the system is close to being critically damped.

shows an oscillatory behavior with a frequency $\sqrt{\Omega^2 - q^2/4}$, where $\Omega = \sqrt{g/\ell}$, and an amplitude that decays with time. At the other extreme, when the damping is large, the behavior is *overdamped*. Here the solution is

$$\theta(t) = \theta_0 e^{-(q/2 \pm \sqrt{q^2/4 - \Omega^2})\,t}, \tag{3.12}$$

which is a monotonic, exponential decay of θ. At the boundary between the underdamped and overdamped regimes, the pendulum is *critically* damped with

$$\theta(t) = (\theta_0 + Ct)e^{-qt/2}. \tag{3.13}$$

Numerical results for $\theta(t)$ in all three cases are shown in Figure 3.4.

While the behavior of our damped pendulum is a bit different from the undamped case considered in the previous section, the results are still not very exciting. We therefore consider the addition of a driving force to the problem. The form of this force will depend on how the force is applied. A convenient choice is to assume that the driving force is sinusoidal with time, with amplitude F_D and angular frequency Ω_D (which is not to be confused with the natural frequency of the simple pendulum, Ω). This might arise, for example, if the pendulum mass has an electric charge and we apply an oscillating electric field. This leads to the equation of motion

$$\frac{d^2\theta}{dt^2} = -\frac{g}{\ell}\theta - q\frac{d\theta}{dt} + F_D\sin(\Omega_D\, t), \tag{3.14}$$

where the last term represents the external driving force. This driving force will pump energy into (or out of) the system, and the externally imposed frequency,

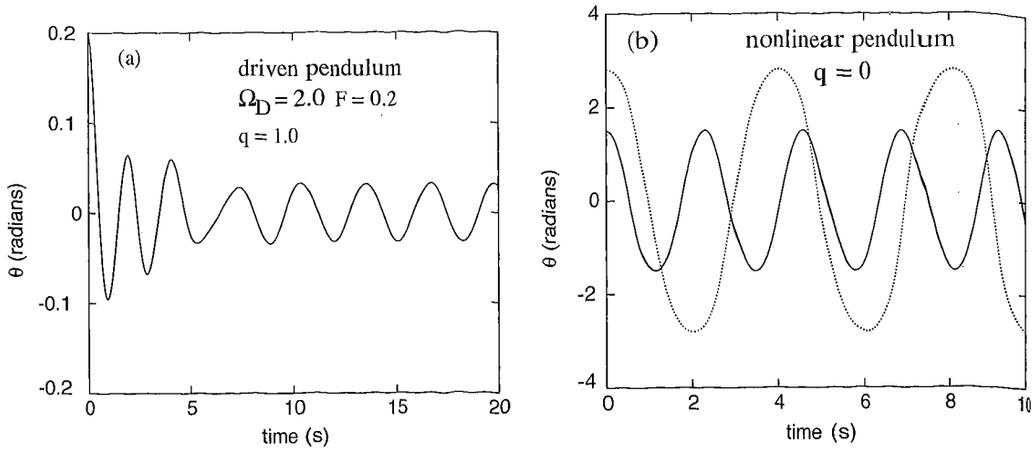

FIGURE 3.5: (a) θ as a function of time for a driven pendulum. (b) θ as a function of time for an undamped pendulum, for two different values of $\theta(0)$. Note that the period is significantly longer when $\theta(0)$ is increased (the dotted curve). For both calculations we used the Euler-Cromer method, with $g = 9.8$ and $\ell = 1.0$.

Ω_D, will "compete" with the natural frequency of the pendulum, Ω, so one might hope to find much richer behavior than we have seen so far.

Alas, it turns out that (3.14) can also be solved analytically, and the behavior is again not very exciting. The steady state solution is

$$\theta(t) = \theta_0 \sin(\Omega_D t + \phi) , \tag{3.15}$$

where the amplitude θ_0 is given by

$$\theta_0 = \frac{F_D}{\sqrt{(\Omega^2 - \Omega_D^2)^2 + (q\,\Omega_D)^2}} . \tag{3.16}$$

This behavior is shown in Figure 3.5(a), which gives some numerical results obtained with the Euler-Cromer method.

The driven, damped pendulum thus undergoes a simple harmonic oscillation with the angular frequency of the driving force, so in some sense its behavior is even simpler than the non-driven case. There is an interesting situation, though, when the driving frequency Ω_D matches the natural angular frequency of the pendulum Ω. In this case of *resonance*, the amplitude θ_0 can become large, especially if the friction is small.

So far, we have assumed that the amplitude of the oscillation is small, and this allowed us to expand the $\sin\theta$ term in (3.1). We will now not make this assumption; this will enable us to treat situations in which the mass swings to large angles or

even all the way around the pivot point of the pendulum.[5] Therefore, we now consider the equation of motion

$$\frac{d^2\theta}{dt^2} = -\frac{g}{\ell}\sin\theta . \tag{3.17}$$

That is, we consider a nonlinear pendulum without friction and without a driving force. Since there is no means of adding to or removing energy from this system, the total mechanical energy is conserved and the pendulum executes a periodic motion. Its period, however, is no longer independent of amplitude. This can be demonstrated analytically, but the mathematics is not simple.[6] However, a numerical approach is straightforward, and some results are shown in Figure 3.5(b). Here we have started our pendulum with some initial displacement (some initial angle $\theta(0)$), and then let it go ($\omega(0) = 0$). The motion is periodic, but it is no longer described by a simple sine or cosine function. You will also notice that (as we just mentioned) the period now depends on the amplitude. When the amplitude is large, the pendulum spends a longer time at its turning points (the points where θ is largest), and this makes the period longer than found for small amplitudes.

All of these results for a more realistic pendulum are in accord with our intuition of how a pendulum should behave. The real fun begins when we put all three of these effects — damping, a driving force, and the nonlinearity — together at the same time. This will be the subject of the next section.

EXERCISES

3.6. Investigate the three regimes of linear pendulum with dissipation (3.10) using the Euler-Cromer (or any other suitable) method. In all three regimes, the dissipation due to friction leads to an exponential damping of the overall energy. Locate the boundary between the overdamped and underdamped regimes numerically, and compare with the analytic result (you can either derive the latter yourself, or find it in a mechanics text such as Marion and Thornton).

3.7. Numerically investigate the linear, forced pendulum with friction of (3.14). Show numerically the existence of the resonance, and confirm the dependence of the resonant amplitude on the driving angular frequency Ω_D, and on the friction parameter q.

3.8. In the nonlinear pendulum of (3.17), use the Euler-Cromer or another suitable method to investigate the relationship between the amplitude and period numerically. Can you give an intuitive argument supporting your results?

[5] To allow such motion in a real pendulum we would have to replace the string in Figure 3.1 with a rigid rod.

[6] This problem can be solved using the conservation of energy and an approach similar to that given in the hint for the anharmonic oscillator of Exercise 3.5. Interested readers can find details in Marion and Thornton (1995). It turns out that the solution involves *elliptic integrals*. These are well-known special functions, but are nonetheless not further reducible in terms of elementary functions. In particular, the period of this system can be expressed as $4\sqrt{l/g}K(\sin(\theta_m/2))$, where θ_m is the maximum angle made by the pendulum and $K(a) = \int_0^{\pi/2} \frac{dx}{\sqrt{1-a^2\sin^2 x}}$ is the complete elliptic integral of the first kind. Its values can be either found in a table (such as in Abramowitz and Stegun in the references), or evaluated numerically using some of the methods discussed in Appendix E. Elliptic integrals occur fairly frequently in physics, particularly in problems related to electricity and magnetism.

3.3 CHAOS IN THE DRIVEN NONLINEAR PENDULUM

Now that we have a numerical method that is suitable for various versions of the simple pendulum problem, and armed with some understanding of what might or might not happen when dissipation, an external driving force, and/or nonlinearity is present, we are ready to take on a slightly more complicated and also more interesting situation. That is, we add all three ingredients which were previously only discussed separately. First, we do not assume the small-angle approximation, and thus do not expand $\sin\theta$ term in (3.1). Second, we include friction of the form $-q(d\theta/dt)$. Third, we add to our model a sinusoidal driving force $F_D \sin(\Omega_D t)$. Putting all of these ingredients together, we have the equation of motion[7]

$$\frac{d^2\theta}{dt^2} = -\frac{g}{\ell}\sin\theta - q\frac{d\theta}{dt} + F_D \sin(\Omega_D t) \; . \tag{3.18}$$

We will call this model for a nonlinear, damped, driven pendulum, (3.18), the *physical pendulum*. It contains some very rich and interesting behavior. We will only be able to touch on a few of its intriguing properties here, although you can explore others through the exercises. Let us begin by examining the behavior of θ as a function of time for several typical cases. First we must construct a program to calculate a numerical solution, since there is no known exact solution to (3.18). Our program is similar in form to the one we used to study the simple pendulum. The only major difference is that we must use a slightly more complicated equation for ω. We again rewrite (3.18) as two first-order differential equations and obtain

$$\frac{d\omega}{dt} = -\frac{g}{\ell}\sin(\theta) - q\frac{d\theta}{dt} + F_D \sin(\Omega_D t) \; , \tag{3.19}$$

$$\frac{d\theta}{dt} = \omega \; .$$

These can be converted into difference equations for θ_i and ω_i as we did in (3.5). These difference equations can then be translated into a program. Below we sketch the subroutine that does the work of calculating θ and ω.

EXAMPLE 3.3 Subroutine `euler_cromer_calculate` for the physical pendulum model

- For each time step i (beginning with $i = 1$), calculate ω and θ at time step $i + 1$.
  - ▷ $\omega_{i+1} = \omega_i - [\,(g/\ell)\sin\theta_i - q\omega_i + F_D \sin(\Omega_D\, t_i)]\,\Delta t$
  - ▷ $\theta_{i+1} = \theta_i + \omega_{i+1}\Delta t$
  - ▷ If θ_{i+1} is out of the range $[-\pi, \pi]$, add or subtract 2π to keep it in this range.

[7]Note that, strictly speaking, the parameter F_D in (3.18) is not the actual force since other factors of m and l also enter. However, F_D is proportional to the driving force, so when we speak of larger drive forces this will mean larger values of F_D, etc.

  - ▷ $t_{i+1} = t_i + \Delta t$
  - ▷ Repeat for the desired number of time steps.

This subroutine is organized much like the `euler_cromer_calculate` routine for our simple pendulum program, but there are several differences of note. First, the equation for ω_{i+1} is more complicated since we have a different equation of motion. Second, we adjust the value of θ after each iteration so as to keep it always between $-\pi$ and π. Recall that our pendulum can now swing all the way around its pivot point, which corresponds to $|\theta| > \pi$. Since θ is an angular variable, values of θ that differ by 2π correspond to the *same* position of the pendulum. This is done because for plotting purposes it is convenient to keep θ in the range $-\pi$ to π. If θ becomes less than $-\pi$, then its value is increased by 2π; likewise, if it becomes greater than $+\pi$, its value is decreased by 2π. This procedure[8] keeps $-\pi \le \theta \le +\pi$. Finally, note that we again use the Euler-Cromer method, but the Runge-Kutta or Verlet methods would also be suitable.

Some typical results for θ and ω as functions of time, as calculated with our program, are shown in Figure 3.6 where we plot the behavior for several different values of the driving force, with all of the other parameters held fixed. With a driving force of zero, the motion is damped and the pendulum comes to rest after at most a few oscillations. These damped oscillations have a frequency close to the natural frequency of the undamped pendulum, Ω, and are a vestige of simple harmonic motion and its damped cousin (3.10). With a small driving force, $F_D = 0.5$, we find two regimes. The first few oscillations are affected by the decay of an initial transient as in the case of no driving force. That is, the initial displacement of the pendulum leads to a component of the motion that decays with time and has an angular frequency of $\sim \Omega$. After this transient is damped away, the pendulum settles into a steady oscillation in response to the driving force. The pendulum then moves at the driving frequency, Ω_D, *not* at its natural frequency, with an amplitude determined by a balance between the energy added by the driving force and the energy dissipated by the damping. This is very similar to the driven, damped, but linear oscillator of (3.14). In a sense, the motion of the pendulum can be viewed as an interplay of the two frequencies Ω and Ω_D, the natural frequency of the pendulum and the frequency of the driving force.

The behavior changes radically when the driving force is increased to $F_D = 1.2$. Now the motion is no longer simple, even at long times. The vertical jumps in θ are due to our resetting of the angle to keep it in the range $-\pi$ to π and thus correspond to the pendulum swinging "over the top." To make this clear, the center plot in Figure 3.6 shows $\theta(t)$ for $F_D = 1.2$, with and without this resetting of the angle. We see that the pendulum does not settle into any sort of repeating steady-state behavior, at least in the range shown here. We might suspect that we have not waited long enough for the transients to decay and that a steady oscillation might be found if we simply waited a little longer. This is not the case; for this

[8]Later on, we will see that this resetting of θ is also useful when we examine the the frequency spectra of these and similar results.

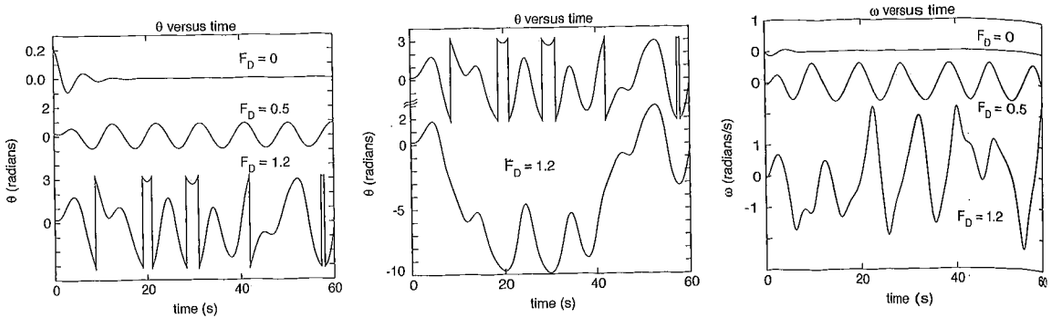

FIGURE 3.6: Left: behavior of θ as a function of time for our driven, damped, nonlinear pendulum, for several different values of the driving force. The vertical "jumps" in θ occur when the angle is reset so as to keep it in the range $-\pi$ to $+\pi$; they do not correspond to discontinuities in $\theta(t)$. Center: behavior of $\theta(t)$ for $F_D = 1.2$ with and without these "resets." Right: corresponding behavior of the angular velocity of the pendulum, ω. The parameters for the calculation were $q = 1/2$, $\ell = g = 9.8$, $\Omega_D = 2/3$, and $dt = 0.04$, all in SI. The initial conditions were $\theta(0) = 0.2$ and $\omega(0) = 0$.

value of the driving force the behavior *never* repeats. This is an example of *chaotic* behavior, which will be our main concern for the rest of this chapter.

It is important to appreciate the behavior illustrated in Figure 3.6. At low drive the motion is a simple oscillation (after the transients have decayed), which would, if we were sufficiently patient, repeat forever. On the other hand, at high drive the motion is chaotic; it is a very complicated nonrepeating function of time. But what does it really mean to be chaotic? Your intuition probably tells you that chaotic behavior is random and unpredictable, and the behavior of our pendulum at high drive certainly has that appearance. However, if the behavior is truly unpredictable, then how was our program able to calculate it? This conundrum can be put another way when we realize that the behavior of our pendulum is described by the differential equation (3.18). From the theory of such equations we know that once the initial conditions (at $t = 0$, for example) are specified, the solution for θ is then *completely determined* for all future times. Indeed, we took this for granted in constructing our program. But how can the behavior be both deterministic and unpredictable at the same time?

We are thus faced with an apparent contradiction between analytic theory (the theory of differential equations) and numerical calculations (our program). Since our only evidence, so far, that the pendulum can be chaotic is from our numerical results, we might be tempted to suspect that we have made some sort of programming error, or that we have somehow misinterpreted the meaning of the numerical results. For example, we could imagine that if we waited long enough, a (predictable) pattern might emerge even at high drive, including at $F_D = 1.2$ in Figure 3.6. Indeed, how could such behavior ever be ruled out? Rather than pursue the question in this way, let us raise another possibility; namely, that the behavior is deterministic *and* unpredictable at the same time! This may seem to be impossible, but we will now show how to reconcile these two, apparently contradictory notions.

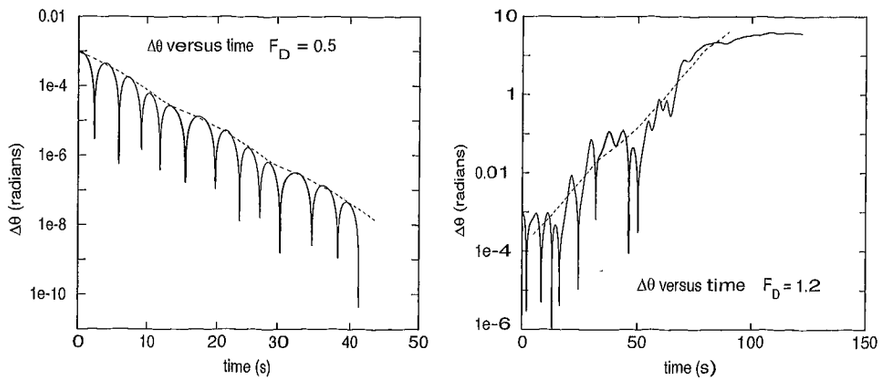

FIGURE 3.7: Results for $\Delta\theta$ from our comparison of two identical pendulums. The parameters were the same as in Figure 3.6. The initial values of θ for the two pendulums differed by 0.001 rad. On the left are results for low drive, while the results on the right were obtained from the chaotic regime. The dashed lines indicate the overall trends, that is, that $\Delta\theta$ decreases approximately exponentially for low drive, and increases roughly exponentially at high drive.

Let us consider the stability of the solutions to our pendulum equation of motion. We imagine that we have two *identical* pendulums, with exactly the same lengths and damping factors. We set them in motion at the same time, with the same driving forces. The only difference is that we start them with *slightly* different initial angles. We thus must calculate the angular positions of two pendulums, θ_1 and θ_2, and we can do this using a program very similar to the one described above (an exercise we will leave to the reader). Some results for $\Delta\theta \equiv |\theta_1 - \theta_2|$ are shown in Figure 3.7 for two different values of the drive amplitude. The smaller value of F_D is the one for which we found simple oscillatory motion in Figure 3.6. To understand these results we first call your attention to the very sharp dips that occur approximately every 3 s. These dips in $\Delta\theta$ occur when one of the pendulums reaches a turning point. $\Delta\theta$ will vanish near each turning point since the trajectories $\theta_1(t)$ and $\theta_2(t)$ must then cross. It is more useful to focus on the plateau regions away from these dips in Figure 3.7. These plateau values of $\Delta\theta$ exhibit a steady and fairly rapid decrease with t. This means that the motion of the two pendulums becomes more and more similar, since the difference in the two angles approaches zero as the motion proceeds. (Indeed, this angular difference decreased by *six orders of magnitude* after about a dozen oscillations.) This in turn means that the motion is *predictable*. If, for some reason, we did not know the initial conditions of one of the pendulums, we could still predict its future motion since our results show that $\theta(t)$ converges to a particular solution (that of the other pendulum). This is what our intuition tells us to expect for predictable, nonchaotic motion.

In contrast, for the larger value of F_D we find that $\Delta\theta$ increases rapidly and irregularly with t; this trend is indicated by the dashed line on the right in Figure 3.7. This is usually described by saying that the two trajectories, $\theta_1(t)$ and

$\theta_2(t)$, *diverge* from one another. Note that this divergence is extremely rapid at short times ($t < 75$ in Figure 3.7). $\Delta\theta$ saturates (i.e., stops changing) at long time periods, but this is only because it has reached a value of order 2π and simply can't get any larger! We have used a logarithmic scale in Figure 3.7, so the increase of $\Delta\theta$ with time is *very* rapid. The irregular variation of $\Delta\theta$ cannot be described by any simple function. However, if we were to repeat this calculation for a range of different initial values of θ_1 (keeping $\Delta\theta(0)$ fixed) and average the results, we would find a much smoother behavior, such as the dashed line in Figure 3.7. This line corresponds to the relation $\log(\Delta\theta) \sim \lambda t$, which implies

$$\Delta\theta \approx e^{\lambda t} . \tag{3.20}$$

It turns out that this functional form for $\Delta\theta$ is very common and the parameter λ is known as a Lyapunov exponent.[9]

For our pendulum the numerical results show that λ is positive at high drive, which means that two pendulums that start with nearly, but not exactly, the same initial conditions will follow trajectories that diverge exponentially fast.[10] Since we can never hope to know the initial conditions or any of the other pendulum parameters exactly, this means that the behavior at $F_D = 1.2$ is for all practical purposes unpredictable. Our system is thus both deterministic and unpredictable. Put another way, a system can obey certain deterministic laws of physics, but still exhibit behavior that is unpredictable due to an extreme sensitivity to initial conditions. *This* is what it means to be chaotic. One more point should be noted from Figure 3.7. The behavior of $\Delta\theta$ can be described by a Lyapunov exponent in both the chaotic and nonchaotic regimes. In the former case $\lambda > 0$, while in the latter, $\lambda < 0$. The transition to chaos thus occurs when $\lambda = 0$.

Now that we have seen how $\theta(t)$ for our pendulum can be unpredictable, you might give up all hope of developing a useful theoretical description of the chaotic regime. However, it turns out that this view is too pessimistic. It is possible to make certain accurate predictions concerning θ, even in the chaotic regime! To demonstrate this we need to consider the trajectory in a different way. Instead of plotting θ as a function of t, let us plot the angular velocity ω as a function of θ. This is sometimes referred to as a *phase-space* plot. Since we have already constructed a program to calculate θ and ω, it is straightforward to modify it to make the desired plot; results for two values of the drive amplitude are shown in Figure 3.8.

[9]In general, systems such as a pendulum possess several different Lyapunov exponents. In order to be chaotic, at least one of these exponents must be positive. The accurate extraction of the values of the Lyapunov exponents from results such as those computed in this section is a somewhat complicated procedure. For one approach to this extraction see Wolf et al. (1985). Also note that logarithmic scales are used in the y-axes in Figure 3.7. This is because of the expectation of exponential behaviors. An exponential function would be displayed as a straight line when a logrithmic y-axis is used and thus it would be easier to spot an exponential dependence on such a plot. In addition, such a plot can clearly display y values that vary over many decades. This is an example of a good plotting strategy mentioned in Chapter 1.

[10]Similar results would be found if the two pendulums had slightly different lengths or driving forces, or if any other of the parameters were different.

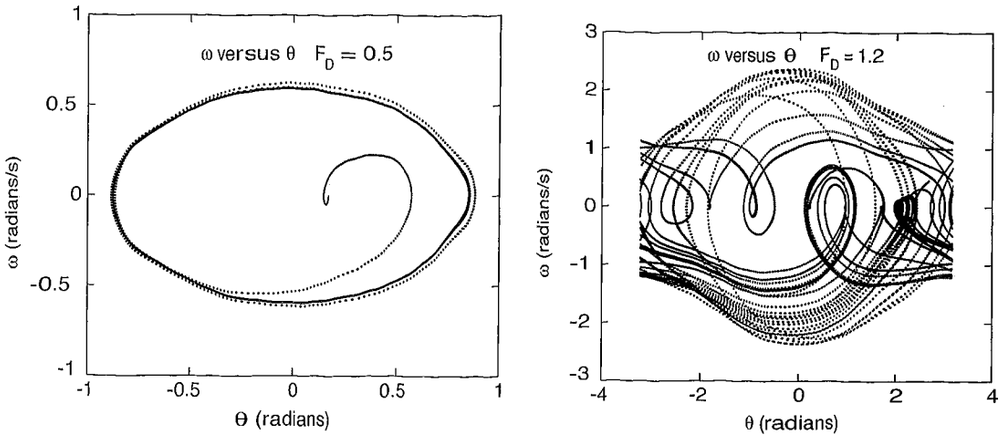

FIGURE 3.8: Results for ω as a function of θ for a pendulum. The parameters were the same as in Figure 3.6. For high drive (on the right), many trajectories go beyond $|\theta| = \pi$ and thus "jump" from $\theta = \pi$ to $\theta = -\pi$, or vice-versa in this plot.

With a small driving force the trajectory in phase space (ω-θ space) is easy to understand in terms of the behavior we found earlier for $\theta(t)$. For short times there is a transient that depends on the initial conditions (in this case we started at $\theta = 0.2$ with $\omega = 0$), but the pendulum quickly settles into a regular orbit in phase space corresponding to the oscillatory motion of both θ and ω. It can be shown that this final orbit is independent of the initial conditions; this is also what our results for the Lyapunov exponent imply. The behavior in the chaotic regime is a bit more surprising. The phase-space trajectory exhibits many orbits that are nearly closed and that persist for only one or two cycles. While this pattern is certainly not a simple one, it is not completely random, as might have been expected for a chaotic system. This is a common property of chaotic systems; they generally exhibit phase-space trajectories with significant structure.

If we examine these trajectories in a slightly different manner we find a very striking result. In Figure 3.9 we show the same type of phase-space graph, but here we plot ω versus θ only at times that are *in phase* with the driving force. That is, we only display the point when $\Omega_D t = 2n\pi$, where n is an integer.[11] This is an example of what is known as a *Poincaré section* and is a very useful way to plot and analyze the behavior of a dynamical system. The motivation for plotting the results in this way can be appreciated from an analogy with the function of a stroboscope. It sometimes happens that we want to examine an object that is rotating at a high rate. A good example is an old-fashioned (vinyl) record as it

[11]When constructing this plot numerically you must be careful to account for the fact that time increases in steps of size Δt. Thus, the points in Figure 3.9 were actually plotted when $|t - 2n\pi/\Omega_D| < \Delta t/2$. Similarly, we could also plot at times corresponding to a fixed phase difference relative to the driving force for analogous results.

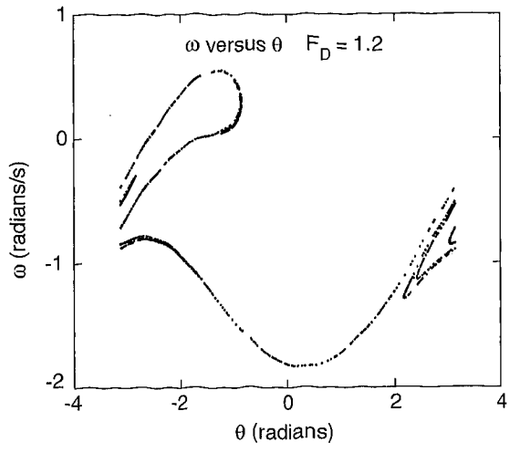

FIGURE 3.9: More results for ω as a function of θ for a pendulum; here we only plot points at times that are in phase with the driving force. The parameters were the same as in Figure 3.6. This surface of points is known as a strange attractor.

is rotated on a record player. When in operation, the record rotates too fast for a human eye to read the label. However, if the record is illuminated with a light source (a stroboscope), that is turned on and off at the frequency of the record player, our eye will receive input only when the record has a particular orientation; as a result we will be able to read the label as if the record were not moving at all. The key point is that things will look simpler when we observe them at a rate (i.e., frequency) that matches the problem. This lesson can be applied to the pendulum by observing the behavior, that is, recording the values of θ and ω, at a rate that matches a characteristic frequency of the system. For a driven pendulum, the obvious candidate for a qualifying frequency is that of the driving force, and this is effectively what we have done in the Poincaré section shown in Figure 3.9. If we had constructed this plot in the nonchaotic regime, with $F_D = 0.5$ for example, it would yield a single point (after allowing the initial transient to decay), since at any particular point of the drive cycle we would always find the same values of θ and ω.

The result of such a stroboscopic plot is very different in the chaotic regime, Figure 3.9. It turns out that except for the initial transient this phase-space trajectory is the same for a wide range of initial conditions. In other words, even though we cannot predict the behavior of $\theta(t)$, we do know that the system will possess values of ω and θ, which put it on this surface of points. The trajectory of our pendulum is drawn to this surface, which is known as an attractor. Actually, there are attractors in both the nonchaotic and chaotic regimes; the single point that would be found with $F_D = 0.5$ would also be an attractor. While the attractors have simple forms in the nonchaotic case, they have a very complicated structure

in the chaotic regime. The "fuzziness" of the chaotic attractor in Figure 3.9 is not due to numerical uncertainties or plotting errors. It is a property of the attractor. Chaotic attractors have a *fractal* structure and are usually referred to as *strange attractors*.[12] We will discuss the nature of fractals at some length in Chapter 7.

There is much more that the damped, nonlinear, driven pendulum can tell us about chaos, and we will explore a few of these lessons in the exercises. Our key results are: (1) it is possible for a system to be both deterministic and unpredictable—in fact, this is what we mean by the term chaos; and (2) the behavior in the chaotic regime is not completely random, but can be described by a strange attractor in phase space. We will amplify and expand on these themes in the following sections.

EXERCISES

3.9. Study the effects of damping by starting the pendulum with some initial angular displacement, say $\theta = 0.5$ radians, and study how the motion decays with time. Use $q = 0.1$ and estimate the time constant for the decay. Compare your result with approximate analytic estimates for the decay time. *Note:* Any of the exercises in the section can be conveniently done with either the Euler-Cromer algorithm or the Runge-Kutta method described in Appendix A.

3.10. Calculate $\theta(t)$ for $F_D = 0.1$, 0.5, and 0.99, with the other parameters as in Figure 3.6. Compare the waveforms, with special attention to the deviations from a purely sinusoidal form at high drive.

3.11. For the three values of F_D shown in Figure 3.6, compute and plot the total energy of the system as a function of the time and discuss the results.

3.12. In constructing the Poincaré section in Figure 3.9 we plotted points only at times that were in phase with the drive force; that is, at times $t \approx 2\pi n/\Omega_D$, where n is an integer. At these values of t the driving force passed through zero [see (3.18)]. However, we could just as easily have chosen to make the plot at times corresponding to a maximum of the drive force, or at times $\pi/4$ out-of-phase with this force, etc. Construct the Poincaré sections for these cases and compare them with Figure 3.9.

3.13. Write a program to calculate and compare the behavior of two, nearly identical pendulums. Use it to calculate the divergence of two nearby trajectories in the chaotic regime, as in Figure 3.7, and make a qualitative estimate of the corresponding Lyapunov exponent from the slope of a plot of $\log(\Delta\theta)$ as a function of t.

3.14. Repeat the previous problem, but give the two pendulums slightly different damping factors. How does the value of the Lyapunov exponent compare with that found in Figure 3.7?

3.15. Study the shape of the chaotic attractor for different initial conditions. Keep the drive force fixed at $F_D = 1.2$ and calculate the attractors found for several different initial values of θ. Show that you obtain the same attractor even for different initial conditions, provided that these conditions are not changed by too much. Repeat your calculations for different values of the time step to be sure that it is sufficiently small that it does not cause any structure in the attractor.

***3.16.** Investigate how a strange attractor is altered by small changes in one of the pendulum parameters. Begin by calculating the strange attractor in Figure 3.9.

[12] Physicists like to use provocative names.

Then change either the drive amplitude or drive frequency by a small amount and observe the changes in the attractor.

***3.17.** Construct a very high-resolution plot of the chaotic attractor in Figure 3.9, concentrating on the region $\theta > 2$ rad. You should find that there is more structure in the attractor than is obvious on the scale plotted in Figure 3.9. In fact, an important feature of chaotic attractors is that the closer you look, the more structure you find. We will see later that this property is related to fractals. It turns out that a strange attractor is a fractal object. *Hint:* In order to get accurate results for a high resolution plot of the attractor, it is advisable, in terms of the necessary computer time, to use the Runge-Kutta method.

3.4 ROUTES TO CHAOS: PERIOD DOUBLING

We have seen that at low driving forces the damped, nonlinear pendulum exhibits simple oscillatory motion, while at high drive it can be chaotic. This raises an obvious question: Exactly how does the transition from simple to chaotic behavior take place? It turns out that the pendulum exhibits transitions to chaotic behavior at several different values of the driving force. We have already observed in Figure 3.6 that one of these transitions must take place between $F_D = 0.5$ and 1.2. However, this transition is not the clearest one to study numerically, so we will instead consider the behavior at somewhat higher driving forces.[13]

Figure 3.10 shows results for θ as a function of time for several values of the driving force calculated using the Euler-Cromer program described earlier. At these high values of the drive the pendulum often swings all the way around its support; this can be seen from the vertical steps in θ as our program resets[14] this angle to keep it in the range $-\pi$ to π. These steps notwithstanding, the behavior in Figure 3.10 is a periodic, repeating function of t in all three cases (after the initial transients have damped away). The drive frequency used here was $\Omega_D = 2/3$ so the period of the driving force was $2\pi/\Omega_D = 3\pi$, and this is precisely the period of the motion found at $F_D = 1.35$. Hence, in this case the pendulum moves with the same frequency as the driving force.

The behavior at $F_D = 1.44$ is a bit more subtle. While we again have periodic motion, the period is now *twice* the drive period. This can be seen most clearly by comparing the θ-t waveforms at $F_D = 1.35$ and 1.44, and noticing that in the latter case the bumps alternate in amplitude. Our pendulum has already surprised us on several occasions, and we might be tempted to add this behavior to our list of pendulum puzzles. However, this surprise is a very special and important one. When a nonlinear system is excited or driven by a single frequency stimulus, the response is, in general, not limited to the driving frequency. If Ω_D is the drive frequency, the nonlinear response will usually contain components at $2\Omega_D$, $3\Omega_D$, etc., at all harmonics. This process is known as mixing and is manifest by the generation of responses at integer multiples of the driving frequency. Such a

[13]The pendulum exhibits an extraordinarily rich behavior, some of which we discuss later. Unfortunately, we only have time to explore a small portion of the chaotic regime here. We will, therefore, limit ourselves to one value of both the drive frequency and damping, and only certain ranges of the drive amplitude. The interested reader is encouraged to investigate other parameter values. Additional results are also described by Baker and Gollub (1990).

[14]This distraction can be avoided by plotting ω instead of θ. We will leave this to the exercises.

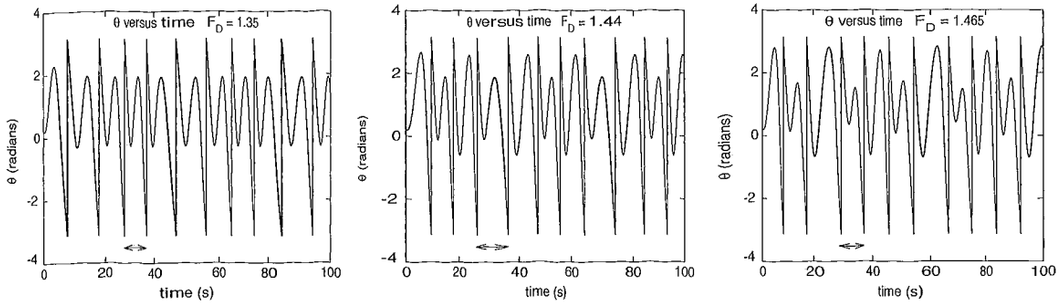

FIGURE 3.10: Results for θ as a function of time for our pendulum for several different values of the drive amplitude. The other parameters were the same as in Figure 3.6 except that here we used a time step of 0.01. The horizontal arrows show the period of the driving force. In the middle plot the period is twice the drive period, since the values at the maxima alternate between $\theta \approx 1.9$ and 2.6. On the right the period is four times the drive period, as the maxima alternate between the values $\theta \approx 1.69$, 2.82, 1.52, and 2.72.

nonlinear response is standard and well understood, and its key property is that it contains frequencies that are equal to or greater than the drive frequency. Hence, the periods of these harmonics will be smaller than the drive period. In contrast, our pendulum is now exhibiting a response at $\Omega_D/2$ (a lower frequency!), a *subharmonic*, which is unlike any standard mixing effect.

Returning to Figure 3.10, a careful look at the results for $F_D = 1.465$ shows that they exhibit a period that is four times the driving period. The pattern should now be evident. If we were to increase the drive amplitude further, the period would double again as the pendulum would switch to a motion that has a period eight times that of the drive. This period-doubling cascade would continue if the drive were increased further.

But if the period keeps on doubling, what about the transition to chaos? A nice way to appreciate how this transition comes about is with what is known as a *bifurcation diagram*. In Figure 3.11 we show a bifurcation diagram for θ as a function of drive amplitude, which was constructed in the following manner. For each value of F_D we have calculated θ as a function of time. After waiting for 300 driving periods so that the initial transients have decayed away, we plotted θ at times that were in phase with the driving force[15] as a function of F_D. Here we have plotted points up to the 400th drive period. This process was then repeated for the range of values of F_D shown in the figure.[16]

To understand the bifurcation diagram we start at $F_D = 1.35$. We have already seen that in this case the motion has the same period as the drive, so if we observe θ at a particular time in the drive cycle we will always find the same

[15]Just as we did in constructing the Poincaré section in Figure 3.9.

[16]We have chosen to study this range of F_D because it exhibits period-doubling in an especially clear manner. Results for other values of F_D are shown by Baker and Gollub (1990), or you can calculate them for yourself.

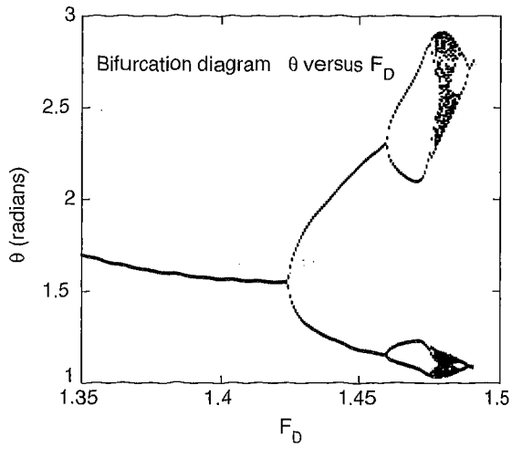

FIGURE 3.11: Bifurcation diagram for our pendulum. The parameters used for the calculation were the same as in Figure 3.10.

value. Our bifurcation diagram thus consists of a single point; there is just one value of θ for this value of F_D, although that point will be plotted many times. We will refer to this as period-1 behavior, since the θ-t waveform has the same period as the driving force. If the motion is period-2, then the values of θ that are plotted will alternate between two values. This is just the alternation we saw at $F_D = 1.44$ in Figure 3.10, and it leads to two points on the bifurcation diagram. The pattern should now be clear: Motion that is period n will yield n points on the bifurcation diagram for that value of F_D. From Figure 3.11 we see that the behavior is period 1 up to approximately $F_D = 1.424$, where there is a transition to period-2 motion. This persists up to the transition to period-4 behavior at $F_D \approx 1.459$. This process continues, although the resolution of our diagram makes it difficult to follow the behavior past period 8. This period-doubling cascade ultimately ends in a transition to chaotic behavior.

We have now obtained at least a qualitative understanding of *how*[17] the transition from regular to chaotic behavior occurs for one particular system, the pendulum, in one particular range of parameters (i.e., drive force, drive frequency, damping strength, etc.). But how general is this behavior? Is it only found in the pendulum, or does it occur in other systems? These are the kinds of questions that physicists often ask. We tend to look for (and like to discover) patterns and principles that occur widely and apply to many different systems. For example, the motion of macroscopic objects can, with only a few exceptions, be described

[17]In this section we have concentrated on the *how* of the period-doubling-route to chaos. In the next section, we will discuss more of the *why*. We will do this using somewhat simpler models, that are often called *iterative maps*. Though perhaps further removed from real physical systems, they offer unique opportunity to investigate the mathematics behind period doubling in great detail.

by Newton's laws of motion. Likewise, classical (as opposed to quantum) electromagnetic phenomena can be described by Maxwell's equations. Because of their near-universal applicability we feel that these "laws" of physics provide us with a better understanding of the world. We don't want to get too philosophical here, and we also don't want to be pressed into a discussion of what the term "understand" really means, but we hope that this gives the reader some appreciation for why it is important to look hard for universal aspects in any problem or result. With that in mind, we now restate the question posed at the beginning of this paragraph. Is the period-doubling route to chaos universal in any way, or do all systems have their own particular way of making this transition?

While there is not yet a complete theory of chaos in the sense of Newton's laws or Maxwell's equations, the answer to this question seems to be the following. Many systems have been found to exhibit chaotic behavior, but there appear to be only a few ways in which the transition from simple to chaotic behavior can occur. The periodic-doubling scenario that we have observed with the pendulum is one of these few known routes to chaos. You can then ask if this periodic-doubling procedure itself has any properties that are universal. The answer to this is yes (why else would we raise the question?!). In the next section we will study a mathematically "stripped down" model called the logistic map, which also exhibits the period doubling route to chaos. The mathematical simplicity of this model will enable us to see why this route to chaos is so common and why many features of the transition are "universal." However, before we discuss the logistic map, it is useful to consider an important property of the period doubling transitions in our pendulum.

Returning to our bifurcation diagram, Figure 3.11, we note that the spacing between period-doubling transitions becomes rapidly smaller as the order of the transition increases. For example, the period-2 regime extends from $F_D \approx 1.424$ to 1.459, while the period-4 regime extends only from about 1.459 to 1.476, and the same trend is found for higher periods.[18] Let us define F_n to be the value of the driving force at which the transition to period-2^n behavior takes place. The shrinkage of the size of the periodic windows can be described by a parameter δ_n, where

$$\delta_n \equiv \frac{F_n - F_{n-1}}{F_{n+1} - F_n} \,. \tag{3.21}$$

The observation that the windows become smaller as n increases means that $\delta_n > 1$. It has been found that as n becomes large, δ_n approaches a constant that is known as the Feigenbaum δ. That is, the rate of shrinkage approaches a constant in the limit $n \to \infty$. Moreover, it turns out that essentially all systems that exhibit the period-doubling route to chaos appear to possess the same value of $\delta \approx 4.669\ldots$. This is one of the universal parameters and features associated with the transition to chaos. There are, as we have hinted above, several other known routes to chaos, and a few of them can also be found in the pendulum. However, rather than making this chapter the story of the pendulum, we will next consider several other chaotic systems.

[18]In order to see this clearly we would need to examine the bifurcation on a much finer scale than in Figure 3.11.

EXERCISES

3.18. Calculate Poincaré sections for the pendulum as it undergoes the period-doubling route to chaos. Plot ω versus θ, with one point plotted for each drive cycle, as in Figure 3.9. Do this for $F_D = 1.4$, 1.44, and 1.465, using the other parameters as given in connection with Figure 3.10. You should find that after removing the points corresponding to the initial transient the attractor in the period-1 regime will contain only a single point. Likewise, if the behavior is period n, the attractor will contain n discrete points.

***3.19.** Calculate Poincaré sections for the pendulum but for a frequency which has *nothing* to do with those intrinsic to the system. For example, you might calculate the Poincaré sections using an angular frequency Ω' that is *irrationally* related to the driving frequency Ω_D (as well as to the natural frequency Ω) for your stroboscopic snapshots. Do the results tell you anything about the system? *Hint:* you will find that the results *look* chaotic even in the periodic regimes. The point is that it is crucial to interrogate the system at a rate that matches one of the intrinsic frequencies of the problem.

3.20. Calculate the bifurcation diagram for the pendulum in the vicinity of $F_D = 1.35$ to 1.5. Make a magnified plot of the diagram (as compared to Figure 3.11) and obtain an estimate of the Feigenbaum δ parameter.

***3.21.** Investigate the bifurcation diagrams found for the pendulum with other values of the drive frequency and damping parameter. Warning: This can easily become an ambitious project!

3.5 THE LOGISTIC MAP: WHY THE PERIOD DOUBLES

In the past few sections we have spent a lot of time studying the chaotic behavior of a pendulum. We now want to look at this problem from a broader perspective and ask the following question: "What does it really take for a system to be chaotic?" That is, what properties must a system have to be chaotic, and can we learn how to predict ahead of time if a particular system is capable of exhibiting chaos? This is a difficult, and extremely important question. In the case of the pendulum, it turns out that chaos is only found when the pendulum is damped, is nonlinear, and is subject to a driving force. All three of these must be present. However, while this fact is useful, it is also important to consider what other simple equations of motion are capable of chaotic behavior.

With these questions in mind, we now consider a rather different type of "system" that is called the *logistic map*. This system can be interpreted as a model for population growth in a collection of animals.[19] The model is defined by the relation

$$x_{n+1} = \mu x_n(1 - x_n) \ . \tag{3.22}$$

One can think of x_n as being the size of the population in generation n, while μ is a parameter related to the amount of food that is available (hence, the value of μ will control the rate of population growth or loss). This "equation of motion" is a *discrete map*, and thus looks rather different from the continuous equations

[19]It also has many other interpretations, as discussed in the article by May (1976). The book by Baker and Gollub (1990) contains a nice introduction to the chaotic behavior of the logistic map.

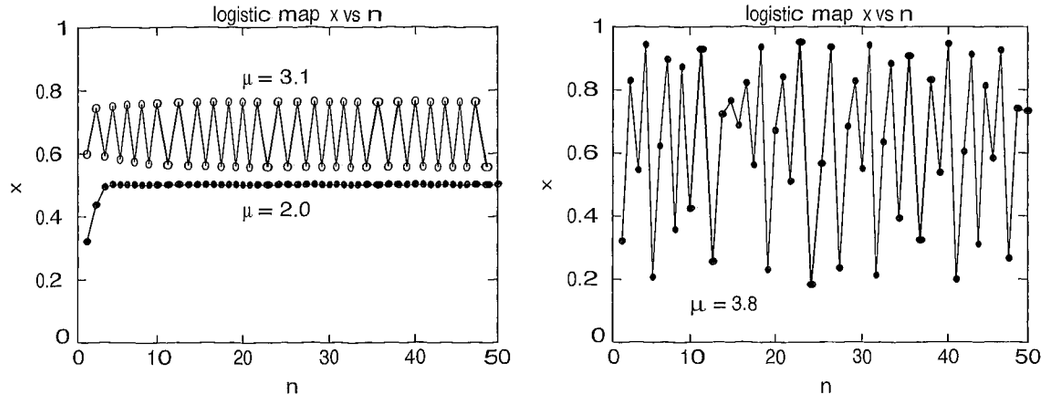

FIGURE 3.12: Behavior of x as a function of n for the logistic map, for several different values of μ. For $\mu = 3.1$ the system is in the period-2 regime, while for $\mu = 3.8$ the behavior is chaotic. Note that the values of x_n are given by the symbols; the connecting lines are simply guides to the eye.

of motion what we are used to seeing in physics. However, you should recognize that in our numerical approaches, such as the Euler method (3.5), we have actually converted a continuous equation of motion (e.g., Newton's law) into a discrete map, so (3.22) is really not that new for us! One advantage of studying the logistic map is that the simplicity of (3.22) will allow us to gain some deep insights into the problem of chaos. However, there is also a potential danger in this general approach. The danger is that the conversion to a discrete map may alter some of the fundamental physics of the problem. For example, it is conceivable that a discrete map may be chaotic, even with the original continuous system is not. This is not the case for any of the systems we study in this book, and we will not pursue this issue here (you can find more on this problem in advanced treatments of chaotic systems). However, the general message (yet again) is that our numerical "solutions" are only approximations to the true behavior.

Let us now consider the general behavior of the logistic map. Figure 3.12 shows the behavior of x_n for several different values of μ. Here we have simply started with a random value of x_0, and used (3.22) to calculate x_1, and then x_2, etc.[20] We see from Figure 3.12 that the logistic map exhibits nonchaotic behavior for small μ, a regime of period-2 behavior for intermediate μ, and chaotic behavior for large μ. We will leave it to the exercises to explore the period doubling route to chaos in this system, and to calculate the associated bifurcation diagram (which bears a striking resemblance to the bifurcation diagram for the pendulum in Figure 3.11). Here we want to explore how the very simple function in (3.22) is able to give such interesting and complex results.

[20]Note that the values of x are restricted to the range between 0 and 1, while μ must lie between 0 and 4.

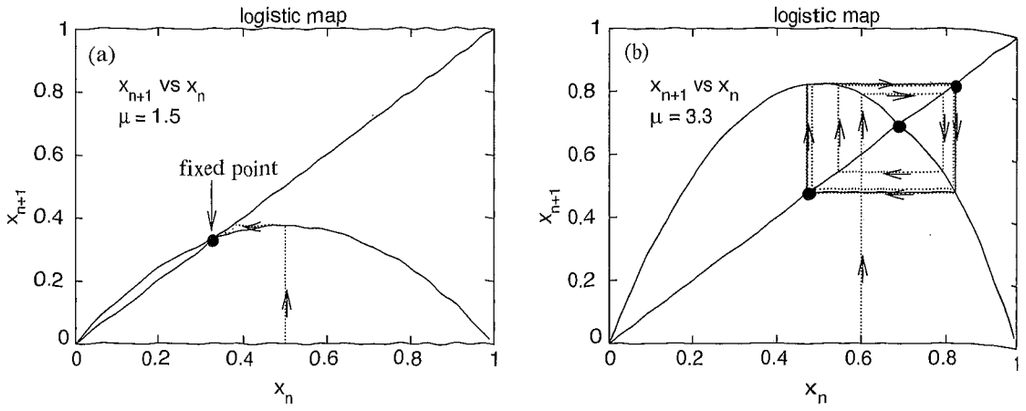

FIGURE 3.13: (a) The logistic map function $f(x)$ for $\mu = 1.5$. The fixed point of the map, x^*, is the point where this function intersects the diagonal line. The dotted lines show the "trajectory" of the system, starting from an initial value $x_0 = 0.5$; the arrows indicate the "direction" that the system moves. Note how the system rapidly approaches the fixed point. (b) For $\mu = 3.3$ the system is in the period-2 regime. There is a fixed point at $x \approx 0.70$, but it is unstable (there is also a trivial fixed point at $x = 0$ for all values of μ). Unless x has this special fixed point value, the system will oscillate between two values of x, as shown here. The dotted lines show the corresponding system trajectory.

Let us first consider the behavior of the logistic map for small values of μ, as found for $\mu = 2.0$ in Figure 3.12. Here the system rapidly approaches a particular value of x that is called a *fixed point*. That is, after many iterations the map "repeats" the same value of x, over and over. If we define the logistic function[21]

$$f(x) = \mu x(1 - x) \ , \tag{3.23}$$

then the fixed points x^* of the map function satisfy the relation

$$x^* = f(x^*) \ . \tag{3.24}$$

You can easily combine (3.23) and (3.24) to find the exact fixed point value(s) x^* as a function of μ. However, it is very instructive to consider the fixed point behavior graphically as shown in Figure 3.13. Here we plot the map function $f(x)$ with $\mu = 1.5$, along with a line with a slope of unity; that is, we have plotted both sides of (3.24). The fixed point solutions are then the values of x at which these two curves intersect. If the value of x somehow gets to a fixed point value, i.e., $x_n = x^*$, then x_{n+1} will repeat the value, and then x_{n+2} will repeat ...

Also drawn as the dotted line in Figure 3.13 is the trajectory of the system starting from an initial value $x_0 = 0.5$. The arrows indicate the path that is taken.

[21]The logistic function $f(x)$ also depends on μ, so it would be more precise to call it $f(x, \mu)$. However, this leads to a somewhat cumbersome notation in what follows, so we will not indicate this dependence explicitly.

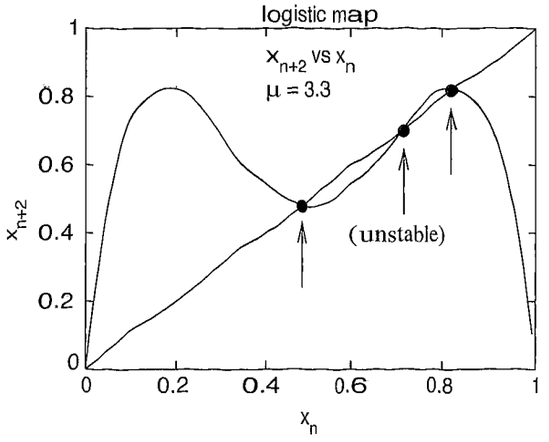

FIGURE 3.14: Second iterate of the logistic map, $f_2(x)$, for $\mu = 3.3$, showing the fixed points. The fixed point near $x \approx 0.70$ is the unstable fixed point associated with the first iterate, $f(x)$.

Starting from the point $[(x_0, 0)]$ on the horizontal axis, the system first moves to the point $[x_0, f(x_0)]$. It then continues on, passing through the points $[x_1, f(x_1)]$, $[x_2, f(x_2)]$, etc., eventually approaching the fixed point at $[x^*, f(x^*)]$.

We can use the same approach to understand the period-2 behavior found for $\mu = 3.3$ in Figure 3.13. The corresponding plot of $f(x)$ and the system trajectory is shown in Figure 3.13(b). There are now three fixed points of the map, and but the system only passes through two of them as it travels along its trajectory. The fixed point at $x^* \approx 0.70$ is unstable. The system avoids this point, and instead cycles between two other values, with one near $x = 0.48$ and the other near $x = 0.82$. These correspond to the period-2 oscillations seen in Figure 3.12.

Deeper insight into the origin of this period-2 behavior can be obtained by considering the so-called "second iterate" of the logistic map. That is, we consider how x_{n+2} depends on x_n. In terms of the logistic function, the second iterate function is

$$f_2(x) = f(f(x)) \ , \tag{3.25}$$

where $f(x)$ is defined in (3.23). When the behavior is precisely period-2, this corresponds to a fixed point of $f_2(x)$, and we can solve for these fixed points just as we found the fixed points of the first iterate, $f(x)$. Figure 3.14 shows a plot of $f_2(x)$ along with the line $x_{n+2} = x_n$. We now find three fixed points, just as in Figure 3.13. One of these (the fixed point in the middle) is the original unstable fixed point of the first iterate $f(x)$. The other two fixed points are stable ones, and describe the period-2 behavior.

This method can be used to study the period-4 regime, by considering the fourth iterate of $f(x)$, etc., for period-8, period-16, and so on. In addition to providing a nice way to analyze these period doubling transitions, this approach

gives insight into the underlying nature of these transitions. Let us examine again the behavior of the first iterate in Figure 3.13, and consider the behavior of $f(x)$ in the vicinity of a fixed point. Near a fixed point we can write

$$f(x^* + \delta x) \approx f(x^*) + f'(x^*)\delta x \,, \tag{3.26}$$

where $f'(x)$ is the derivative of $f(x)$. If the system starts a short distance from the fixed point, i.e., we start at a value of x for which $\delta x = x - x^*$ is small, we can apply (3.26). We can see that if the derivative $|f'(x^*)| < 1$, then the system will move towards x^* as the map is iterated, while if $|f'(x^*)| > 1$, the system will move away from the fixed point. Hence, the behavior is controlled by the magnitude of this derivative. As μ is varied, the value of $f'(x^*)$ will also vary, so we can now see how, in a mathematical sense, the fixed point can be made unstable. At the same time, this leads to two additional fixed points for $f_2(x)$, and this is why the system is driven into a period-2 regime. Thus, we are now able to see *why* the system undergoes a period-doubling transition. Indeed, this general line of attack can be extended to the higher period transitions, and is described in the paper by Feigenbaum (1978). Moreover, we can now see why these period doubling transitions can be *universal*; i.e., why many details of the behavior can be the same in different systems. The idea here is that the logistic function, $f(x)$, is representative of the map function for a very general system. Near the transitions, such functions will generally have a smooth (i.e., Taylor expansion) form that is the same as that of $f(x)$. Hence, the nature of the fixed points, their stability, the second iterate functions, etc., will all be basically the *same* for many different systems. This is why the chaotic properties of very different systems, including the logistic map and the nonlinear pendulum, can be *universal*.

EXERCISES

3.22. The logistic map undergoes successive period doubling as μ is increased from below 3 and finally develops a fully chaotic behavior at $\mu \approx 3.56$. It is interesting to compute the bifurcation diagram for the logistic map (the analog of Figure 3.11 for the pendulum). Use numerical results for the logistic map to estimate the value of the Feigenbaum δ parameter and compare it with that quoted above for the pendulum. The article by May (1976) and the book by Baker and Gollub (1990) contain good introductions to the logistic map.

3.23. Calculate the trajectories of the logistic map, as shown in Figure 3.13, for different values of μ. It is especially interesting to do this in the period-4, period-8, ... regimes, and also when the system is chaotic.

***3.24.** Iterative maps are often used to produce what are called "pseudo-random" numbers. In this exercise, you will look at the behavior of such maps and investigate what makes them suitable for this purpose.

(a) First, consider the following,

$$x_{i+1} = [\alpha x_i 2^n + \beta] \,(\mathrm{mod}\; 2^n)\, /2^n \,, \tag{3.27}$$

where mod(2^n) indicates the remainder after division by 2^n. Here $0 \leq x_i < 1$ and n, α, and β are suitable integers. Fix n (say, to 8) and investigate the properties of the maps for various values of α when the $\beta = 0$ and again when $\beta = 1$. Also consider the effect of different initial values x_0.

(b) Next, consider a variation of the above where discrete steps are introduced by using the int(x) function (which takes the greatest integer not exceeding x):

$$x_{i+1} = [\mathrm{int}\,(x_i 2^n)\,\alpha + \beta] \,(\mathrm{mod}\; 2^n)\, /2^n \,. \tag{3.28}$$

Do the same as in part (a). Try values of α which are even, and also odd numbers of the forms $8m \pm 1$ and $8m \pm 3$. You might be interested to know that this is very similar to the standard random number generator function found in many software packages, and is called the multiplicative congruential method. In most practical generators one takes advantage of the integer arithmetic overflows, but here you should avoid them. The quality of the random numbers depends on the choice of α, β, and n. While there are some theoretical results for how to choose these parameters to produce "good quality" random numbers, much is only known empirically. See Appendix F and also Knuth (1998) and Hamming (1987) for more on this.

3.6 THE LORENZ MODEL

The two models that we have considered so far in this chapter — the pendulum and the logistic map — are both very simple systems, yet they exhibit extremely rich behavior. It is thus not surprising that other slightly more complicated systems are also capable of chaotic behavior. When we think of chaotic or unpredictable behavior, an example that naturally comes to mind is the weather. Because of the economic importance of having accurate weather predictions, a good deal of effort has been devoted to this problem. While much of this effort has gone into computer modeling of Earth's atmosphere, much has also been devoted to understanding the weather problem from a more fundamental point of view. It was work of this kind by the atmospheric scientist E. N. Lorenz (1963) that provided a major contribution to the modern field of chaos.

Lorenz was studying the basic equations of fluid mechanics, which are known as the Navier-Stokes equations; they can be thought of as Newton's laws written in a form appropriate for a fluid. These are a complicated set of differential equations that describe the velocity, temperature, density, etc., as functions of position and time, and they are very difficult to solve analytically in cases of practical interest. Of course, this is just the type of problem where a computational approach can be useful, and that is precisely what Lorenz did. The specific situation he considered was the Rayleigh-Bénard problem, which concerns a fluid in a container whose top and bottom surfaces are held at different temperatures. It had long been known that as the difference between these two temperatures is increased, the fluid can undergo transitions from a stationary state (no fluid motion) to steady flow (nonzero flow velocities that are constant in time, also referred to as convection) to chaotic flow. Lorenz did his work more than 40 years ago, so the computational power available to him was not very impressive by today's standards. This prompted him to consider a greatly simplified version of the Navier-Stokes equations as applied to this particular problem. Indeed, he grossly oversimplified the problem as he

reduced it to only three equations

$$\frac{dx}{dt} = \sigma (y - x) , \tag{3.29}$$

$$\frac{dy}{dt} = - x z + r x - y ,$$

$$\frac{dz}{dt} = x y - b z .$$

These are now known as the Lorenz equations (or equivalently, the Lorenz model).[22] As noted above, the Navier-Stokes equations, from which those in (3.29) are derived, involve the state of the fluid as a function of position and time. Hence, a complete description of the Rayleigh-Bénard problem must involve a *large* number of variables. The Lorenz variables x, y, and z are derived from the temperature, density, and velocity variables in the original Navier-Stokes equations, and the parameters σ, r, and b are measures of the temperature difference across the fluid and other fluid parameters. However, it is not particularly useful to insist on interpreting x, y, and z in that manner, since the simplifications made in reducing the problem to only three variables means that we cannot expect our results to apply to any real system. Rather, the behavior exhibited by these equations is indicative of the *type* of behavior that could be expected of the Rayleigh-Bénard problem or any other problem involving the Navier-Stokes equations. For brevity we shall often refer to the latter as the weather problem. Any behavior we find in the Lorenz model will certainly be found in the weather problem. Moreover, it makes strategic sense to attack the Lorenz model first, since if we can't solve that, we would have no hope of making headway on the weather problem.

With this in mind, we plunge ahead and consider solutions to the Lorenz equations. They are just three, coupled, differential equations that are very similar to those we have already encountered in connection with the pendulum [for example, (3.4)]. We will, therefore, not discuss the program construction in detail; it is basically the same approach we employed in the previous sections, but with the pendulum equation of motion replaced by the Lorenz equations. However, we will make a few general comments about the numerical aspects of the problem. We saw in our work on the pendulum that the Euler method does not conserve energy for oscillatory problems. The Lorenz equations exhibit oscillatory solutions for certain parameter values, which could cause us to worry about using the Euler method. We might, therefore, want to use the Euler-Cromer method here, but since that algorithm is designed for second-order differential equations, it is not directly applicable to the Lorenz model. However, it turns out that the Euler algorithm can actually be used to treat the Lorenz problem, for the following reason. Several of the terms in the Lorenz equations play the same role as the damping term in the pendulum equations of motion, while other terms are analogous to the driving

[22] While these do not appear to resemble our pendulum's equation of motion, the two systems are both nonlinear (note the terms involving products such as xz and xy), and as we saw with the pendulum, this is very important.

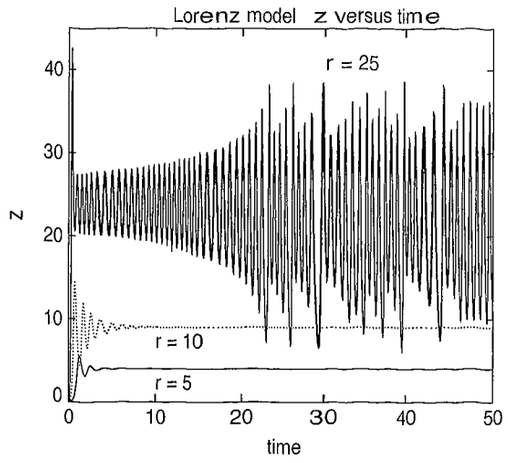

FIGURE 3.15: Variation of the Lorenz variable z as a function of time. The calculation was performed using the Euler method with a time step of 0.0001. The initial conditions were $x = 1$, $y = z = 0$.

force. If the time step in the Euler algorithm is sufficiently small, the energy lost (or added) through the error terms associated with the Euler method can be made much smaller than the energy lost to the effective damping, or added by the effective driving force. In this situation the Euler method provides an accurate solution, as can be verified directly by simply repeating the Euler calculation with different time steps, or by comparing with the solution generated with the Runge-Kutta method. This exercise, which we will leave to the reader, reveals that the Euler solution is accurate for the time steps we have employed in the computations described below. This is another example of a point we made earlier; the suitability of an algorithm depends upon the problem.

Returning to the Lorenz problem, there are three parameters in (3.29), σ, b, and r, and the behavior one finds depends on their values. We will follow custom (and also Lorenz [1963]) and use $\sigma = 10$ and $b = 8/3$. According to some authors these values correspond to cold water, but given the highly simplified nature of the model you shouldn't take this claim seriously! The parameter r is a measure of the temperature difference between the top and bottom surfaces of the fluid. For small r the effective force on the fluid is small in the sense that there is very little heat carried by the fluid. As r increases this force increases, so r plays a role analogous to the drive amplitude, F_D, in the pendulum problem. Results for z as a function of time are shown in Figure 3.15, which shows the behavior at three different values of the force r (x and y exhibit qualitatively similar behavior). At $r = 5$ there is an initial transient, and after it decays away z is a constant, independent of t. The same behavior is seen at $r = 10$, although the transient takes a little longer to decay. These two cases correspond to steady convective motion in the original fluid; in this process the warm fluid produced at the bottom surface of the container rises

and the cooler fluid returns from the top. This steady convection is the analog of regular nonchaotic motion of the pendulum. The behavior is completely different at $r = 25$. Here the initial transient is roughly periodic, but it gives way to an irregular, that is, chaotic time dependence after $t = 20$ or so. There are not many exact results available for the Lorenz model, but it is known that the transition from steady convection to chaotic behavior takes place at $r = 470/19 \approx 24.74$. This is consistent with our numerical results, although we have not attempted to locate this transition accurately here; we leave that for the exercises!

The chaotic behavior seen at $r = 25$ after the initial transient has decayed certainly appears to be very random and unpredictable. However, we learned in dealing with the pendulum that looks can be deceiving. In that case we found that a Poincaré section can reveal underlying regularities that are not obvious from the time dependence alone. With this motivation we consider how to construct such a phase-space plot for the Lorenz model. The situation here is a little more complicated than that of the pendulum, since we now have three variables to deal with, x, y, and z, as opposed to only two in the pendulum problem (θ and ω). There are several ways to proceed. Perhaps the simplest way is to imagine that x, y, and z are coordinates in some abstract space and recognize that we are dealing with a trajectory in this space. We can then obtain a projection of this trajectory[23] by simply plotting z as a function of x (for example); this gives a projection onto the x–z plane. Such a projection for the chaotic case $r = 25$ is shown in Figure 3.16. In this trajectory the system undergoes approximately periodic oscillations (roughly circular orbits) on one side of the line $x = 0$, then moves to the opposite side of this line and undergoes a new series of oscillations, etc.

The phase-space plot in Figure 3.16 certainly gives some hints of an underlying regularity, but we would like to have more than hints. With the pendulum we saw that the Poincaré sections in the chaotic regime reveal the attractors in a particularly clear way, as with the strange attractor in Figure 3.9. Might there be a similar sort of underlying attractor for the Lorenz model? You will recall that to construct a Poincaré section for the pendulum we plotted ω as a function of θ at times that were in phase with the driving force. Hence, we essentially used the driving force as a timekeeper, which told us when to make the measurement. However, in the Lorenz model there is no direct analog to this drive force with its sinusoidal time dependence, so we must take a slightly different approach. We already mentioned that the Lorenz variables x, y, and z can be viewed as specifying the trajectory of a particle moving in three dimensions. It is then natural (or at least it was to Lorenz!) to consider two-dimensional slices through this trajectory. To be more specific, we show on the left in Figure 3.17 a plot of z versus y when

[23]It is difficult to present a full three-dimensional trajectory in this book, but nowadays it is not very hard to find ways to do so on a video monitor. In addition to using one of the many 3D visualization applications, some computer languages even have specialized extensions to accommodate 3D plotting. Many of these will even allow you to rotate and zoom around the plot at will. A case in point is a system called *VPython* (the Visual module of a language called *Python*). It is highly recommended that you try to plot and view the Lorenz model trajectory in full three dimensions using one of these methods, particularly as the time evolves and the butterfly-like trajectory gradually becomes filled in.

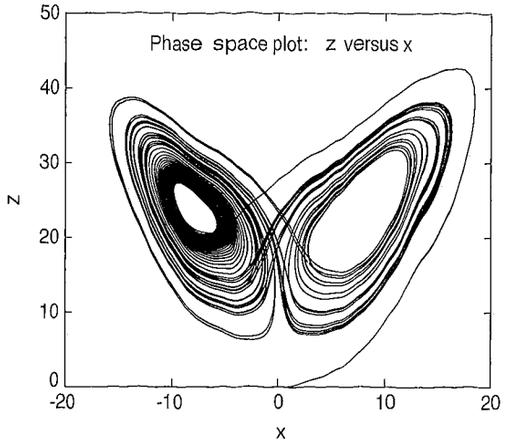

FIGURE 3.16: Trajectory of the Lorenz model projected onto the x–z plane, with $r = 25$. This was calculated using the Euler method with a time step of 0.0001 and the initial conditions $x = 1$, $y = z = 0$.

$x = 0$.[24] In our trajectory language, we are simply plotting the places where the trajectory intersects the y–z plane. The results in Figure 3.17 were obtained with $r = 25$, which, as we have already seen, places us in the chaotic regime. We see from the figure that even though the behavior is strongly chaotic, there is a very high degree of regularity in the phase-space trajectory. This attractor surface in phase space can be shown to be independent of the initial conditions. Hence, while the time-dependent behavior [e.g., $z(t)$] is unpredictable, we *can* predict with certainty that the system will be found somewhere on the attractor surface in phase space.

In the previous section we studied the period-doubling route to chaos in the pendulum. The Lorenz model exhibits this route to chaos, and several others as well. A complete study of the model would take us too long here, so we refer the interested reader to Sparrow (1982), an entire *book* devoted to the Lorenz model. Here we will only explore one of the chaotic transitions exhibited by the model. Figure 3.18 shows the behavior of z at two values of r. At $r = 160$ we see periodic oscillations. While the waveform of these oscillations is certainly not simple, they are stable and persist forever. This corresponds to period-1 behavior, and is analogous to the results we found for the pendulum. If we were to examine the behavior as r is made smaller, we would observe period-doubling and eventually chaos (see the exercises for more on this). However, let us instead consider what happens as r is increased; this is also shown in Figure 3.18. The motion is seen to be approximately periodic for many cycles of oscillation, but these periodic stretches

[24]Since t can take on only discrete values in our simulations, we can only determine that the system has crossed the plane $x = 0$ at some instant between two adjacent time steps. We then interpolate the position to construct the phase-space plots.

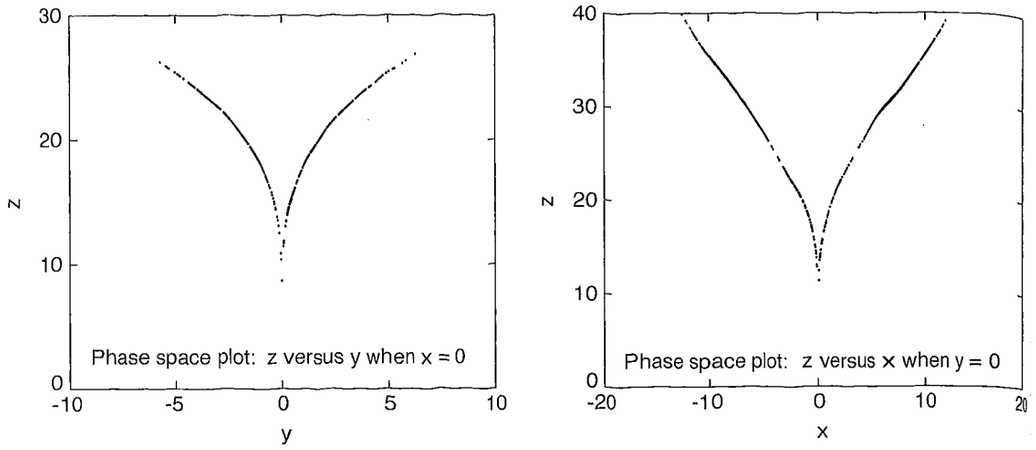

FIGURE 3.17: Phase-space plots for the Lorenz model with $r = 25$, calculated with a time step of 0.0001. Left: z versus y, with points plotted only when $x = 0$. Right: z versus x, with points plotted only when $y = 0$. The points were recorded only after $t = 30$, to allow for the decay of initial transients.

are interrupted by chaotic interludes (hiccups?). The behavior is thus chaotic, but in a sense it is only barely chaotic.

This is known as the intermittency route to chaos, and can be pictured as follows. Let r_c be the value of r at which this transition occurs. For r less than r_c the behavior is perfectly periodic, as found with $r = 160$. For values of r that are just a little beyond the transition, in our case just a little larger than r_c, the behavior is *almost* periodic with only an occasional chaotic interlude. As we go farther and farther into the chaotic regime these interludes occur more and more often, until eventually the underlying periodic behavior is unrecognizable. As we approach r_c, but still stay inside the chaotic regime, there are fewer and fewer interludes spaced farther and farther apart. At the transition the spacing between the interludes becomes infinitely long; that is, they no longer occur, and we are left with periodic motion.

The Lorenz model is a very rich and interesting chaotic system, and we will explore it in further detail in the exercises. Before we leave this topic we have a few comments concerning what the behavior of the Lorenz model implies about the weather problem. We have seen that the Lorenz model can exhibit chaotic behavior. Since it is a special case of the Navier-Stokes equations, we must expect that chaos is a general property of virtually all fluid systems. The weather problem is concerned with a complicated fluid system, our atmosphere, so we reach the not very surprising conclusion that the weather is a chaotic problem. From what we have learned about the extreme sensitivity of chaotic systems to initial conditions, we know that predicting the weather must therefore be an *inherently* difficult problem. Suppose

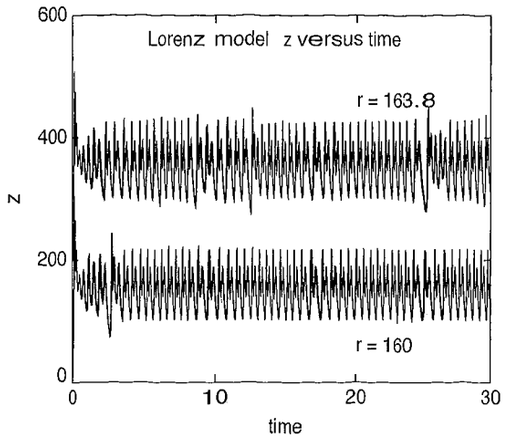

FIGURE 3.18: Variation of the Lorenz variable z as a function of time, for high values of r. Calculated using the Euler method with a time step of 0.0001. The results here show that the system is periodic at $r = 160$, and that it starts to develop some irregular features at $r = 163.8$. The threshold value of r at which this transition to chaos is observed is very sensitive to the accuracy of the approximation. So, a more accurate calculation (e.g., with a higher order Runge-Kutta method) can yield a slightly different threshold value of r. However, the general result is the same, with periodic behavior at small r, changing to chaotic behavior as r is increased.

that we construct an extremely detailed computer model of the atmosphere (this problem is not in the exercises). The model would take all atmospheric conditions, including the temperature, wind velocity, etc., as functions of position around the world at some particular time as input parameters, and then calculate how these conditions vary with time. However, assuming that the atmosphere is in its chaotic regime (and it appears that it is), any slight error in any of the initial conditions would rapidly lead to an enormous error in the predictions. This conclusion should be no surprise; we all know how bad current weather forecasts can be, and these are based largely on computer models (or the human equivalent!). This situation led to the butterfly metaphor that appeared in the title of a talk by Lorenz, "Predictability: Does the Flap of a Butterfly's Wings in Brazil Set Off a Tornado in Texas?"[25] This is just another reference to the extreme sensitivity of chaotic systems to their initial conditions.

EXERCISES

***3.25.** Study period-doubling in the Lorenz model by examining the behavior for $r \leq 160$. Calculate the bifurcation diagram and extract the value of Feigenbaum's δ parameter. You should find a value similar to that calculated for the pendulum.

[25] Given at a meeting of the American Association for the Advancement of Science in 1972. It seems fitting that the trajectory in Figure 3.16 bears some resemblance to a butterfly.

Hint: While this problem can be done using the Euler method, it is probably advisable, in order to conserve computer time, to use the Runge-Kutta algorithm.

3.26. Continue the previous problem, and construct the phase-space plots as in Figures 3.16 and 3.17 in the different regimes.

3.27. Show that the Poincaré sections in Figure 3.17 are independent of the initial conditions. For example, compare the attractor found for $x(0) = 1$, $y(0) = z(0) = 0$ with that found for $x(0) = 0$, $y(0) = z(0) = 1$.

***3.28.** Estimate qualitatively the Lyapunov exponent for a few trajectories of the Lorenz model near the transition to chaos at $r = 24.74\ldots$. Try to observe this exponent change from negative in the nonchaotic regime, to positive in the chaotic regime.

***3.29.** Explore the intermittency route to chaos for $r \geq 163$ in more detail. Begin by calculating z as a function of time for different values of r. Try $r = 163$ (which should be in the nonchaotic regime), and several larger values up to $r = 165$ or so. For the larger values of r you should observe chaotic "hiccups" like those found in Figure 3.18. Next calculate the average time between these hiccups and study how it diverges as the transition to chaos is approached. While the idea here is easy to explain, writing a program to detect hiccups is a bit tricky. One way to accomplish this is to construct a histogram of times between adjacent maxima in $z(t)$. In the oscillatory (nonchaotic) regime these times will all be the same. An odd value signals a hiccup.

3.7 THE BILLIARD PROBLEM

So far we have considered two different chaotic systems, and you are probably willing to believe that there are many more. To get an appreciation for the different kinds of behavior that can be found, and also the common threads that run through this behavior, we will consider one more chaotic model in this chapter. Here we consider the problem of a ball moving without friction on a horizontal table. We imagine that there are walls at the edges of the table that reflect the ball perfectly and that there is no frictional force between the ball and the table. We can think of this as a billiard ball that moves without friction on a perfect billiard table.[26] The ball is given some initial velocity, and the problem is to calculate and understand the resulting trajectory. This is known as the stadium billiard problem.

Except for the collisions with the walls, the motion of the billiard is quite simple. Between collisions the velocity is constant so we have

$$\frac{dx}{dt} = v_x \,, \qquad (3.30)$$

$$\frac{dy}{dt} = v_y \,,$$

where v_x and v_y change only through collisions with the walls. These equations can be solved using our usual Euler algorithm. Note that since the velocity is constant (except during the collisions), the Euler solution gives an exact description of the

[26] We will ignore any complications associated with the angular momentum of the ball, so it is better to think of this as a particle sliding on a frictionless sheet of ice. It would thus be more accurate to term this the "hockey puck" problem, but the name billiard is already firmly attached to the model.

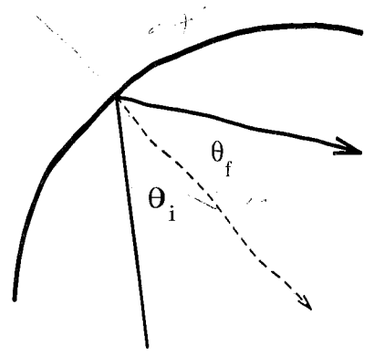

FIGURE 3.19: Geometry for perfect reflection of the billiard from a wall. The angle of incidence is equal to the angle of reflection, $\theta_i = \theta_f$.

motion across the table. The most difficult part of the calculation is the treatment of the collisions. Since we have assumed that they are perfectly elastic, the reflections will be mirrorlike, which means that the angle of incidence will be equal to the angle of reflection. These angles are defined in terms of the incoming and outgoing velocity vectors, and the vector normal to the wall at the location of the collision. This geometry is shown in Figure 3.19, where we have drawn a curved wall; our arguments apply just as well to a straight wall.

A numerical solution for the billiard's motion thus consists of two parts. First, when the billiard is away from the wall its motion is described by (3.30). These equations of motion are used to integrate forward in time, calculating x and y as functions of time. After each time step we must check to see if there has been a collision with one of the walls, that is, if the newly calculated position puts the billiard off the table. When this happens the program must backtrack to locate the position where the collision occurred. There are several ways to do this. One way is to back the billiard up to the position at the previous time step and then use a much smaller time step [for example, a factor of 100 smaller than the time step used to initially integrate (3.30)], so as to move the billiard in much smaller steps. When the billiard then goes off the table (again), we take the location after that iteration to be the point of collision.[27] After locating the collision point, we need to do a little vector manipulation. The initial velocity vector $\vec{v}_i \equiv (v_x, v_y)$ is already known, since v_x and v_y are known. We must next obtain the unit vector normal to the wall at the point of collision, $\hat{n}$. It is then useful to calculate the

[27] This approach will always yield a collision point that is off the table by a small amount. We can imagine other ways to locate the collision point, but in most cases they will never locate the collision point exactly. We have found that the approach described here yields results that are essentially identical to other methods for locating the collision point. A different method will be considered in the exercises.

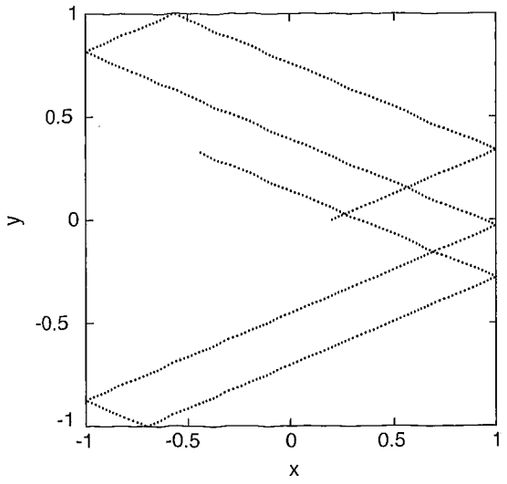

FIGURE 3.20: Trajectory of a billiard on a square table. Only the first few reflections are shown. The billiard started at $x = 0.2$, $y = 0$ with a speed of unity and with the velocity directed toward the upper right of the table. The time step was 0.01.

components of $\vec{v}_i$ parallel and perpendicular to the wall. These are just

$$\begin{aligned} \vec{v}_{i,\perp} &= (\vec{v}_i \cdot \hat{n})\,\hat{n}\,, \\ \vec{v}_{i,\parallel} &= \vec{v}_i - \vec{v}_{i,\perp}\,. \end{aligned} \tag{3.31}$$

Once we have the components of $\vec{v}_i$ we can reflect the billiard. A mirrorlike reflection reverses the perpendicular component of velocity, but leaves the parallel component unchanged (we'll leave it to the reader to show that this makes $\theta_f = \theta_i$ in Figure 3.19). Hence, the velocity after reflection from the wall is

$$\begin{aligned} \vec{v}_{f,\perp} &= -\,v_{i,\perp}\,, \\ \vec{v}_{f,\parallel} &= v_{i,\parallel}\,. \end{aligned} \tag{3.32}$$

Some results are given in Figure 3.20, which show the first few bounces for a billiard on a square table. When (if) you write your own program for this problem, a graphical display of the trajectory is extremely useful in finding, and fixing, any errors. Two strong tests of the program are that the reflections should indeed be mirrorlike (usually referred to as *specular*), and that the energy, which is all kinetic for this problem, should be conserved. The trajectory on a square table is, as we might infer from Figure 3.20, very regular; it has a very simple predictable pattern. This is confirmed in Figure 3.21, which shows such a trajectory over a much longer time period.

Another way to graphically capture the regularity of the trajectory is with yet another phase-space plot. In Figure 3.21 we show a plot of v_x versus x, but

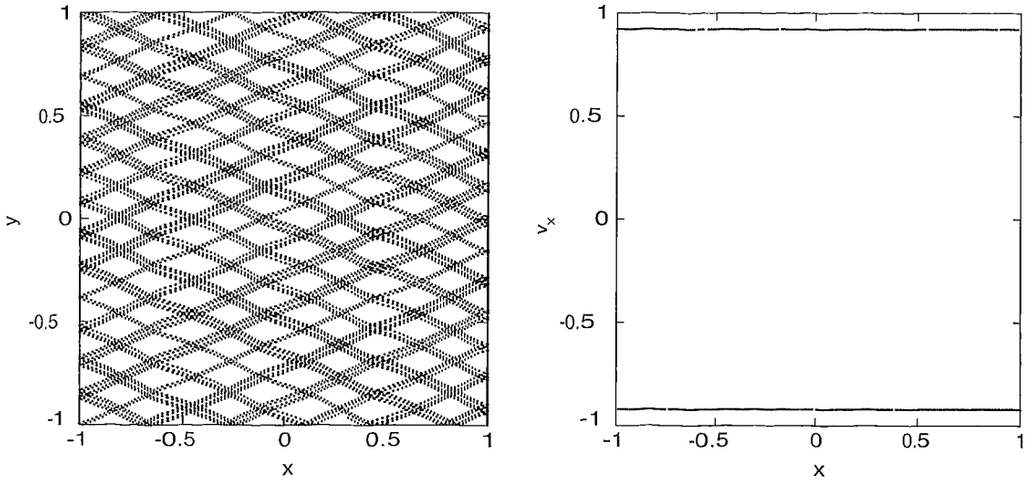

FIGURE 3.21: Left: trajectory of a billiard on a square table. This is a continuation of the trajectory shown in Figure 3.20. Right: corresponding Poincaré section derived from the trajectory shown on the left. Note that the phase-space plot was obtained from a much longer run of the program than was used for the trajectory plot. There are a few gaps visible in the phase-space plot; these would be filled in if the program were run for a longer period of time.

here we have not plotted every point of the phase-space trajectory. Rather, we have constructed another type of Poincaré section by plotting the points only when the billiard crosses the $y = 0$ axis.[28] We find two horizontal lines here; the billiard trajectories are all parallel to one of two different directions, so only two different values of v_x occur. Since the billiard can cross the $y = 0$ axis anywhere, the values of x in this plot vary continuously from -1 to $+1$.

The behavior of the billiard gets more interesting when we consider other table shapes. There are many possibilities; here we will consider only one, the so-called stadium shape, which can be described as follows. Imagine a circular table of radius $r = 1$, as shown on the left side of Figure 3.22. Now cut the table along the x axis, and pull the two semicircular halves apart (along y), a distance $2\alpha r$. Then fill in these two open sections with straight segments. Thus $\alpha = 0$ yields a circular table, while nonzero values of α give a table with a more traditional stadium shape. Figure 3.22 compares trajectories for a circular table with those for a table with $\alpha = 0.01$. While the trajectories depend on the initial conditions (the initial values of x, y, and $\vec{v}$), the results for the circular table are always highly symmetric. On the other hand, the trajectory for the $\alpha = 0.01$ stadium is much more complicated and is definitely not symmetric, except for very special initial conditions (such conditions were not used in Figure 3.22).[29] This should remind you of chaotic motion.

[28] This should remind you of how we dealt with the Lorenz model.

[29] Examples of such special, nonchaotic initial conditions are $x(0) = y(0) = 0$, with $\vec{v}$ parallel to either the x or y axis.

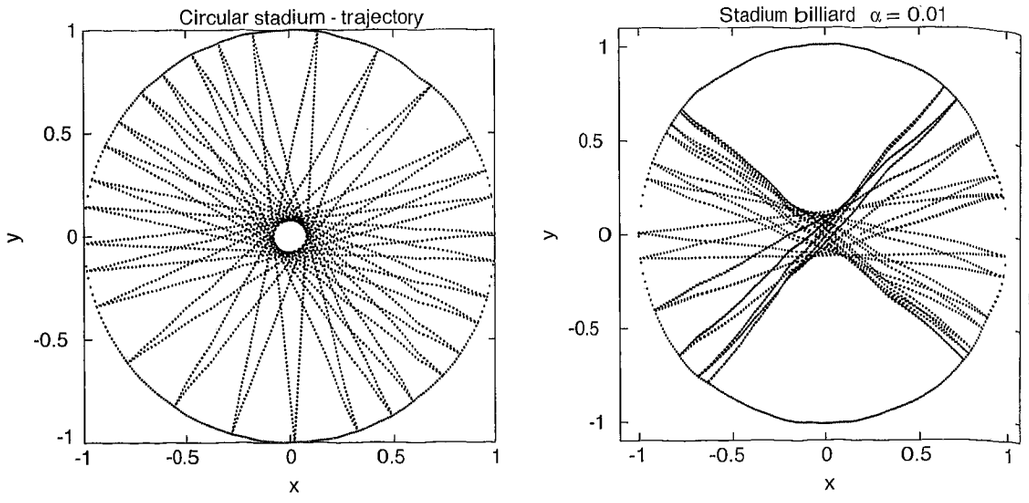

FIGURE 3.22: Left: trajectory of a billiard on a circular table; right: trajectory of a billiard on a stadium-shaped table with $\alpha = 0.01$.

The corresponding phase-space plots of v_x versus x (constructed as in Figure 3.21) are shown in Figure 3.23. The very ordered pattern for the circular table confirms our impression from the trajectories, that this is a nonchaotic system. However, for the $\alpha = 0.01$ stadium the phase-space plot is somewhat reminiscent of the chaotic attractor we found for the pendulum problem; it is indeed chaotic. Two more phase-space plots for other stadium shapes are shown in Figure 3.24, and both are seen to be chaotic.

A hallmark of a chaotic system is an extreme sensitivity to initial conditions. This property is also found in the billiard problem, as can be seen if we calculate the trajectories of two billiards with slightly different initial conditions. An example is shown in Figure 3.25 where we plot the distance between two billiards as a function of time. The billiards were on a chaotic table ($\alpha = 0.01$) and were given the same initial velocities, but were started a distance 1×10^{-5} apart (recall that the table has a radius of approximately 1 unit). The billiard separation shows a very sharp dip after about every one time unit. These dips occur when the billiards collide with the walls, as this causes their trajectories to cross. The overall separation is seen to increase very rapidly with time (note the logarithmic scale). The divergence of these trajectories can be described by a Lyapunov exponent, as we found for the pendulum.[30]

A remarkable feature of our results for the billiard problem is that the chaotic behavior is evident even for very small values of α. It turns out that the stadium billiard is chaotic for *any* nonzero value of α. In fact, only tables with very high

[30]To calculate the Lyapunov exponent quantitatively we would would have to average the behavior over different initial conditions, so as to smooth out the irregularities in Figure 3.25.

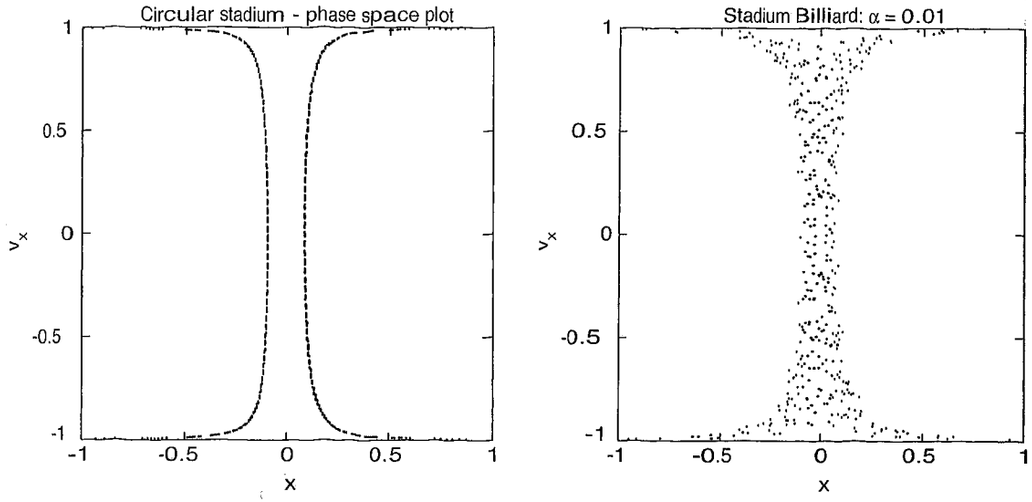

FIGURE 3.23: Phase-space plots for the trajectories shown in Figure 3.22. Left: for a circular-shaped table; right: for a stadium-shaped table with $\alpha = 0.01$. These were constructed by plotting points only when $y = 0$.

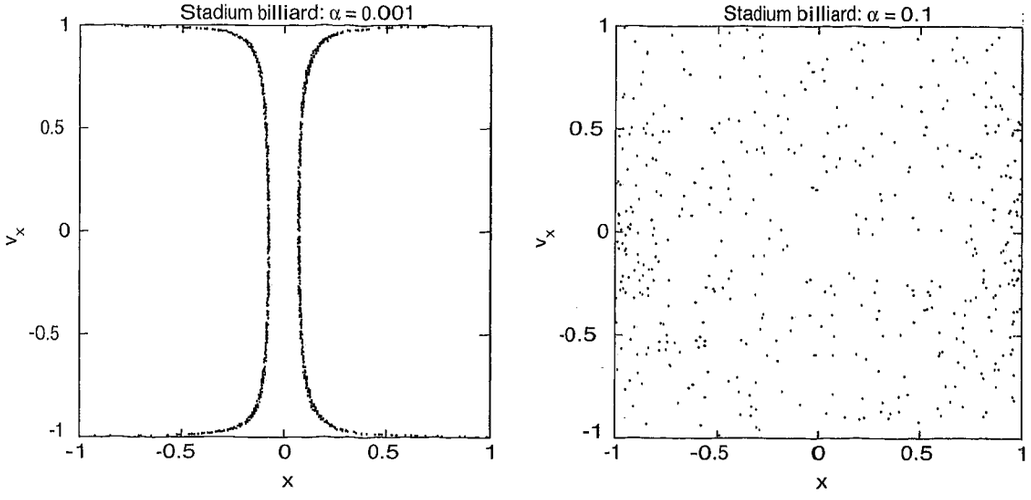

FIGURE 3.24: Phase-space plots for two more stadium-shaped tables. Left: for a table with $\alpha = 0.001$; right: table with $\alpha = 0.1$.

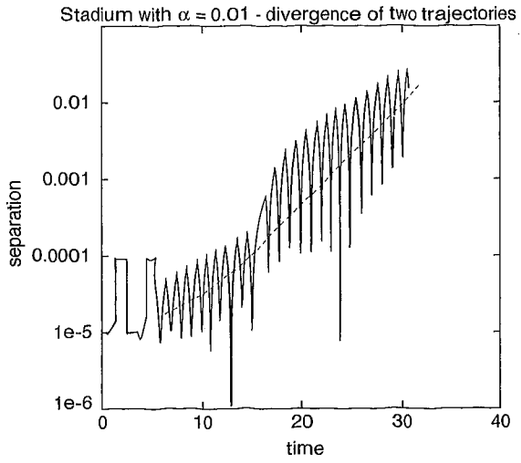

FIGURE 3.25: Divergence of the trajectories of billiards started at slightly different initial conditions, for a stadium-shaped table with $\alpha = 0.01$. The dashed line is drawn to emphasize the rapid overall increase of the separation with time. The initial separation of the billiards was 1×10^{-5}.

symmetry are nonchaotic. The billiard problem may be relevant for describing the motion of gas molecules in a container. Our results suggest that for any realistically shaped container (i.e., any shape that is not extremely symmetric, such as the perfectly circular table) such motion is likely to be chaotic and thus unpredictable. This finding will be relevant to our discussion of entropy and the approach to equilibrium in Chapter 7.

EXERCISES

3.30. Investigate the Lyapunov exponent of the stadium billiard for several values of α. You can do this qualitatively by examining the behavior for only one set of initial conditions for each value of α you consider, or more quantitatively by averaging over a range of initial conditions for each value of α.

***3.31.** Study the behavior for other types of tables. One interesting possibility is a square table with a circular interior wall located either in the center, or slightly off-center. Another possibility is an elliptical table.

***3.32.** The key part of a program for the billiard program is the treatment of collisions with the wall of the stadium, and one way of doing this was described above. Another way is to use the exact solution of (3.30) to compute the trajectory and then solve analytically (using the equation that specifies the perimeter of the stadium) for the location of the collision. Write a program that uses this method and compare your results with those given in this section.

3.8 BEHAVIOR IN THE FREQUENCY DOMAIN: CHAOS AND NOISE

Our intuitive ideas concerning what it means to be chaotic usually include some connection with terms such as *random*, *unpredictable*, and *noisy*. We have already

explored the first two notions; in this section we consider how chaotic behavior is connected with noise. For this we require several tools for dealing with time-dependent signals. These tools are discussed in Appendix C and rely on the Fourier transform.[31]

Our goal in this section is to Fourier analyze the time-dependent signals obtained in our simulations of the damped, nonlinear pendulum in Section 3.3. We will consider only the signals associated with the angular position of the pendulum, $\theta(t)$, although the same sort of analysis could be used with the angular velocity, $\omega(t)$. Such a signal can, in general, be a complicated function of time. Nevertheless, we show in Appendix C how it can always be decomposed into component waveforms that are simple sines and cosines. If you choose to write your own program to calculate this Fourier decomposition, we recommend that you use the fast Fourier transform (FFT) algorithm described in Appendix C (another option is to use the FFT routine in your favorite software package).

In this section we will be concerned only with the frequency spectrum associated with $\theta(t)$, which can be derived using its power spectrum. Here the term *power* is used in the following sense. Typical signals of interest include the amplitudes of pressure waves, electrical voltages, and light waves. In such cases the square of the amplitude of a particular frequency component of the signal is proportional to the *intensity* of the signal at that frequency, which is in turn proportional to the power carried by the signal. An examination of the intensity as a function of frequency leads to the *power spectrum* discussed in Appendix C. This term is commonly used, even in cases (such as the present one) where the connection with power and energy is not direct.[32]

The power spectra of several pendulum waveforms[33] are shown in Figures 3.26 and 3.27, where we show the power spectrum of $\theta(t)$ as a function of frequency for different values of F_D. The area under each peak in the spectrum is proportional to the effective power, that is, the sum of the squares of the corresponding Fourier components of the signal. At low drive, $F_D = 0.5$, the pendulum is in a period-1 state, in which the $\theta(t)$ waveform is very close to a simple sine wave. The FFT result shows a single peak at the frequency of this sine wave, that is, at the drive frequency. This is completely analogous to what we found for the FFT of a sine wave in Appendix C. At somewhat higher drive $F_D = 0.95$, the behavior is again period-1, and we see that the power spectrum is again dominated by a single peak at the drive frequency. We also notice a very small peak at approximately three

[31] Readers who are not familiar with the concept of Fourier analysis should review Appendix C before tackling this section.

[32] Although with the pendulum, the power spectrum of $\theta(t)$ will be closely connected with the kinetic energy of the system.

[33] In calculating these power spectra, it it useful to use the time series data for $\theta(t)$ which have been shifted to keep the pendulum angle in the range $|\theta| < \pi$, as explained in connection with Figure 3.6. Using the unshifted values of θ from Section 3.3 can lead to large low frequency components in the power spectrum (you might think about why this is so). Also, in this and other situations where you are using Fourier transforms, it is essential to first formulate a strategy about what value of the time step Δt should be used, and over how many time steps you should sample the time series. Although a small Δt may be required to accurately track the time evolution of the nonlinear system (making the Nyquist frequency very high), it might be useful to obtain a high frequency resolution, which requires a long time series.

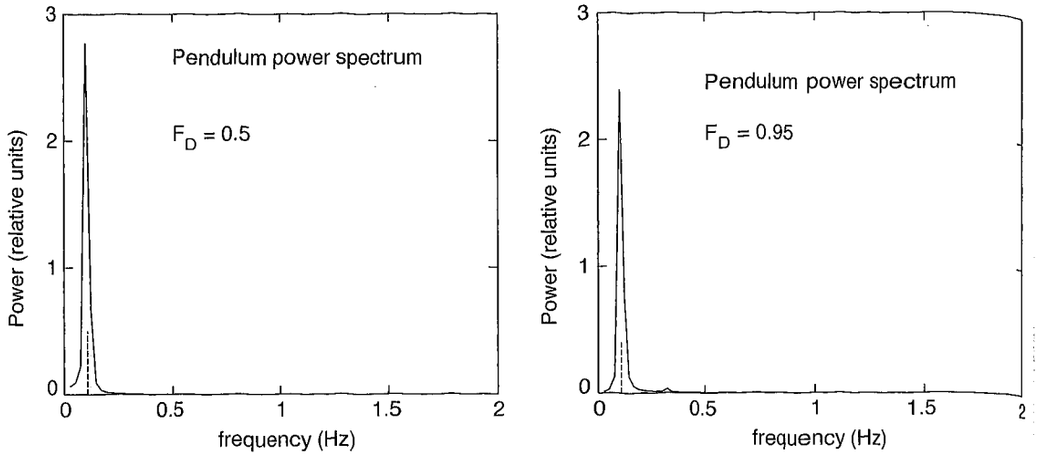

FIGURE 3.26: Fourier analysis of the results for $\theta(t)$ for the nonlinear pendulum at different values of the driving force. At $F_D = 0.5$ and $F_D = 0.95$ the pendulum is in the period-1 regime. The dashed lines indicate the drive frequency.

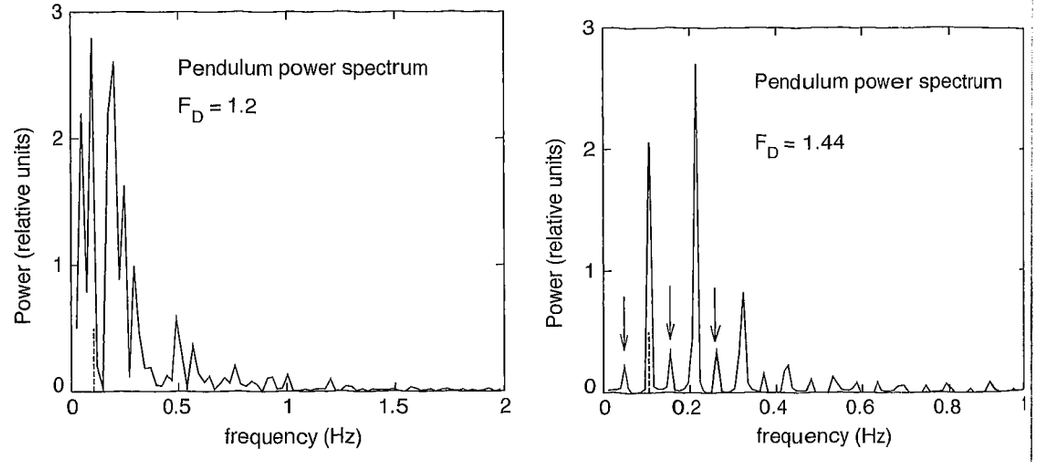

FIGURE 3.27: Left: With $F_D = 1.2$ the pendulum is chaotic. Right: When $F_D = 1.44$ the pendulum is in the period-2 regime. The dashed line indicates the drive frequency. The arrows on the right indicate the subharmonic (period-doubled) component, which appears at half the drive frequency, and some of its harmonics.

times the drive frequency (≈ 0.3 Hz). This peak is not a plotting error! It is produced by the nonlinearity of the waveform at this drive and is an example of the phenomenon of nonlinear mixing we mentioned earlier. The most interesting result is found in the chaotic regime, $F_D = 1.2$ (on the left in Figure 3.27). The spectrum is now very complicated as the power is broadly distributed over a wide range of frequencies. This is just the noise that we intuitively expect to find in a chaotic system.

It is also interesting to examine the power spectra when the pendulum undergoes period-doubling on its way to the chaotic regime. Results from the period-2 regime are shown on the right in Figure 3.27. There is a large peak at the drive frequency $\Omega_D/2\pi \approx 0.1$ Hz, with additional peaks at integer multiples of this frequency, as we again have the nonlinear mixing observed earlier. However, there is now a strong component at half this frequency, ≈ 0.05 Hz. This corresponds to a component with twice the period and is, therefore, the result of *period-doubling*. A similar analysis can be used to examine the behavior in the period-4, period-8, etc., regimes. If the behavior is period-n, there will be a spectral component at a frequency $1/n$ times the drive frequency. Hence, spectral analysis reveals the period-doubling route to chaos in an extremely clear manner.

The key result of this section is that much can be learned about the behavior of a system by examination of its frequency spectrum. Here we have used this approach to study the pendulum in and near its chaotic states. In later chapters we will use the same method in connection with several other problems.

EXERCISES

3.33. In Figure 3.26 we saw that at a relatively high drive, $F_D = 0.95$, there was a small, but noticeable response of the pendulum at three times the frequency of the driving force. Calculate the size of this component as a function of the drive force in the range $F_D = 0.95 - 1.00$. Try also to observe a component at five times the drive frequency. The process in which these signals at multiples of the drive frequency are produced is an example of mixing.

3.34. Analyze the behavior of the nonlinear pendulum in the period-4 regime and show that the spectral component with the lowest frequency has a frequency of one-fourth the drive frequency.

***3.35.** We saw in connection with Figures 3.10 and 3.11 that every time a period-doubling threshold is crossed a new subharmonic component is added to the $\theta(t)$ waveform. The size of this component can be readily extracted using the Fourier transform. Calculate $\theta(t)$ for values of the drive amplitude near the period-2 transition in Figure 3.11. Then use the FFT to obtain the amplitude of the period-2 component as a function of F_D. Try to determine the functional form that describes the way in which this amplitude vanishes at the transition.

3.36. Analyze the power spectrum of $\omega(t)$ of the nonlinear pendulum for different values of the driving force.

3.37. Calculate the frequency spectra for the waveforms $z(t)$ for the Lorenz model. Compare the behavior in the chaotic, nonchaotic, intermittent, and period-doubled regimes.

REFERENCES

[1] M. Abramowitz and I. A. Stegun, Editors, 1964, *Handbook of Mathematical Functions with Formulas, Graphs, and Mathematical Tables.* National Bureau of Standards, Washington, DC.

[2] A. Cromer, "Stable Solutions using the Euler Approximation," Am. J. Phys. **49**, 455 (1981). Discusses the Euler-Cromer method, and shows analytically that it conserves energy for oscillatory problems.

[3] G. L. Baker and J. P. Gollub, 1990, *Chaotic Dynamics: an Introduction,* Cambridge University Press, Cambridge. A very readable introduction to chaotic behavior in simple systems. Discusses the logistic map extensively and also has a nice description of the damped nonlinear pendulum.

[4] M. J. Feigenbaum, "Quantitative Universality for a Class of Nonlinear Transformations," J. Stat. Phys. **19**, 25 (1978). A mathematical but quite readable account of how universality in iterative maps come about.

[5] R. Hamming, 1987, *Numerical Methods for Scientists and Engineers,* Dover, New York. Chapter 8.

[6] R. C. Hilborn, 1994, *Chaos and Nonlinear Dynamics: An Introduction for Scientists and Engineers,* Oxford University Press, Oxford. A thorough introduction to chaos. Goes into much more depth than we have had space to discuss in this chapter.

[7] D. E. Knuth, 1998, *Art of Computer Programming, Vol. 2,* Addison-Wesley, Reading.

[8] E. N. Lorenz, "Deterministic Nonperiodic Flow," J. Atmos. Sci. **20**, 130 (1963). The classic treatment of the Lorenz equations.

[9] J. B. Marion and S. T. Thornton, 1995, *Classical Dynamics of Particles and Systems,* Brooks-Cole, Belmont. One of the standard texts of classical mechanics at a slightly higher level than typical in lower division mechanics courses. Standard discussions of oscillators as well as of coupled oscillators can be found here.

[10] R. M. May, "Simple Mathematical Models with very Complicated Dynamics," Nature **261**, 459 (1976). A nice introduction to iterated maps, such as the logistic map (3.22).

[11] F. C. Moon, 1992, *Chaotic and Fractal Dynamics,* John Wiley & Sons, Redwood City. A nice discussion of a wide variety of chaotic systems. The overall level is somewhat more advanced than our treatment.

[12] C. Sparrow, 1982, *The Lorenz Equations: Bifurcations, Chaos, and Strange Attractors,* Springer-Verlag, New York. Devoted entirely to the Lorenz model.

[13] A. Wolf, J. B. Swift, H. L. Swinney, and J. A. Vastano, "Determining Lyapunov Exponents from a Time Series," Physica **16D**, 285 (1985). Estimating Lyapunov exponents quantitatively is not an easy task. This paper describes one way to do it.